

Cubic-quartic regularization models for solving polynomial subproblems in third-order tensor methods

Coralia Cartis^{*,†} and Wenqi Zhu^{*,‡}

December 25, 2023

Abstract

High-order tensor methods for solving both convex and nonconvex optimization problems have recently generated significant research interest, due in part to the natural way in which higher derivatives can be incorporated into adaptive regularization frameworks, leading to algorithms with optimal global rates of convergence and local rates that are faster than Newton’s method. On each iteration, to find the next solution approximation, these methods require the unconstrained local minimization of a (potentially nonconvex) multivariate polynomial of degree higher than two, constructed using third-order (or higher) derivative information, and regularized by an appropriate power of the change in the iterates. Developing efficient techniques for the solution of such subproblems is currently, an ongoing topic of research, and this paper addresses this question for the case of the third-order tensor subproblem. In particular, we propose the CQR algorithmic framework, for minimizing a nonconvex Cubic multivariate polynomial with Quartic Regularisation, by sequentially minimizing a sequence of local quadratic models that also incorporate both simple cubic and quartic terms. The role of the cubic term is to crudely approximate local tensor information, while the quartic one provides model regularization and controls progress. We provide necessary and sufficient optimality conditions that fully characterise the global minimizers of these cubic-quartic models. We then turn these conditions into secular equations that can be solved using nonlinear eigenvalue techniques. We show, using our optimality characterisations, that a CQR algorithmic variant has the optimal-order evaluation complexity of $\mathcal{O}(\epsilon^{-3/2})$ when applied to minimizing our quartically-regularised cubic subproblem, which can be further improved in special cases. We propose practical CQR variants that judiciously use local tensor information to construct the local cubic-quartic models. We test these variants numerically and observe them to be competitive with ARC and other subproblem solvers on typical instances and even superior on ill-conditioned subproblems with special structure.

1 Introduction and Problem Set-up

In this paper, we consider the unconstrained nonconvex optimization problem,

$$\min_{x \in \mathbb{R}^n} f(x). \quad (1)$$

Here, $f : \mathbb{R}^n \rightarrow \mathbb{R}$ is p -times continuously differentiable and bounded below, $p \geq 1$. Recent research [4; 10; 12; 28] showed that some optimization algorithms demonstrate superior worst-case complexity bounds when they leverage high-order derivative information of the objective function alongside

^{*}The order of the authors is alphabetical; the second author (Wenqi Zhu) is the primary contributor.

[†]Mathematical Institute, Woodstock Road, University of Oxford, Oxford, UK, OX2 6GG. cartis@maths.ox.ac.uk

[‡]Mathematical Institute, Woodstock Road, University of Oxford, Oxford, UK, OX2 6GG. wenqi.zhu@maths.ox.ac.uk

adaptive regularization techniques. In these optimization methods, a polynomial local model $m_p(x_k, s)$ plays a crucial role as an approximation to $f(x_k + s)$ at the current iterate x_k . Then, x_k is iteratively updated by $s_k \approx \operatorname{argmin}_{s \in \mathbb{R}^n} m_p(x_k, s)$, and $x_{k+1} := x_k + s_k$, whenever sufficient objective decrease is obtained. This process continues iteratively until an approximate local minimizer of f is found, satisfying conditions such as $\|\nabla_x f(x_k)\| \leq \epsilon_g$ and $\lambda_{\min}(\nabla_x^2 f(x_k)) \geq -\epsilon_H$.

The construction of the model m_p relies on the p th-order Taylor expansion of $f(x_k + s)$ at x_k

$$T_p(x_k, s) := f(x_k) + \sum_{j=1}^p \frac{1}{j!} \nabla_x^j f(x_k)[s]^j,$$

where $\nabla^j f(x_k) \in \mathbb{R}^{n^j}$ is a j th-order tensor and $\nabla^j f(x_k)[s]^j$ is the j th-order derivative of f at x_k along $s \in \mathbb{R}^n$. To ensure a local model that is bounded from below and to maintain convergence in the optimization method, we introduce an adaptive regularization term¹ into T_p ,

$$m_p(x_k, s) = T_p(x_k, s) + \frac{\sigma_k}{p+1} \|s\|^{p+1}, \quad (\text{AR}p \text{ Model})$$

where $\sigma_k > 0$. Notably, when $p = 1$, this equation represents the steepest descent model, while $p = 2$ corresponds to a Newton-like model. In this paper, our primary focus lies on the case where $p = 3$. This construction, as articulated in (AR p Model), corresponds to the subproblem in the well-known adaptive regularization algorithmic framework AR p [4; 10; 12]. Within AR p , the parameter σ_k dynamically adjusts to ensure progress towards optimality across iterations. Under Lipschitz continuity assumptions on $\nabla^p f(x)$, AR p requires no more than $\mathcal{O}\left(\max\left[\epsilon_g^{-\frac{p+1}{p}}, \epsilon_H^{-\frac{p+1}{p-1}}\right]\right)$ evaluations of f and its derivatives to compute a local minimizer to accuracy (ϵ_g, ϵ_H) for first-order and second-order criticality. The theoretical result highlights that as we increase the order p , the evaluation complexity bound improves. For instance, the AR3 algorithm has evaluation complexity² of $\mathcal{O}\left(\max\epsilon_g^{-4/3}, \epsilon_H^{-2}\right)$ which is better than the worst-case performance compared to first/second-order methods.

1.1 Literature Review for Minimizing AR3 Model

When $p = 3$, the subproblem m_3 is a potentially nonconvex, quartically-regularized multivariate polynomial,

$$m_3(x_k, s) = f(x_k) + \nabla_x f(x_k)^T s + \frac{1}{2} \nabla_x^2 f(x_k)[s]^2 + \frac{1}{6} \nabla_x^3 f(x_k)[s]^3 + \frac{\sigma_k}{4} \|s\|^4. \quad (\text{AR3 Model})$$

Efficiently minimizing $m_3(s)$ is important for the overall performance of the AR3 algorithm. Consequently, our primary objective is to devise specialized algorithms tailored for the optimization of m_3 . While it is worth noting that finding the global minimum of m_3 is an NP-hard problem [5; 24], our goal here is to efficiently identify a local minimizer of $m_3(s)$. Importantly, it has been established in previous work [12] that obtaining a local minimizer of $m_3(s)$ is sufficient to ensure the favorable computational complexity of the AR3 algorithm.

Finding ways to efficiently minimize m_3 remains an open question and is the main focus of this paper. While there have been some previous algorithms related to minimizing the AR3 subproblems, they often lack explicit handling of the tensor term or the fourth-order regularization. Schnabel et al. [15; 36; 37] considered solving unconstrained optimization using third-order tensor local models

¹Unless otherwise stated, $\|\cdot\|$ denotes the Euclidean norm in this paper.

²This complexity metric excludes the computational cost associated with minimizing the subproblem (AR p Model).

without the regularization term. Birgin et al. [3] introduced a variant of the AR3 algorithm, comparing its performance with AR2/ARC. In the case of a convex m_3 , Nesterov proposed a series of second-order methods for its minimization [28; 29; 30; 31; 32; 33]. These methods utilize various convex optimization tools, including Bregman gradient methods, high-order proximal-point operators, and iterative minimization of convex quadratic models with quartic regularization. Recently, Cartis and Zhu [14; 38] introduced the Quadratic Quartic Regularisation (QQR) method. QQR approximates the third-order tensor term of the AR3 model with a linear combination of quadratic and quartic terms, resulting in (possibly nonconvex) local models that can be solved to global optimality. In this paper, we aim to enhance the previous approach by explicitly incorporating third-order terms. For local minimization of m_3 , local first and second-order methods originally designed for optimizing $f(x)$ can also be applied directly, including ARC (also known as AR p with $p = 2$).

In addition to the works mentioned above, there is a body of literature on polynomial optimization for (globally) minimizing certain quartic polynomials. In specific cases where the polynomial exhibits convexity or can be expressed as a sum of squares (SOS) of polynomials, semidefinite programming (SDP) methods have been shown to converge to global minimizers [1; 21; 22; 23]. Recently, [1] proposed a high-order Newton's method that uses SDP to construct and minimize an SOS convex approximation to the p th-order Taylor expansion of the objective function. However, when such conditions do not hold, alternative methods become necessary. In [35], a global descent algorithm is proposed for finding a global minimizer of such quartic polynomials in two variables ($n = 2$). Burachik et al. [2; 5] proposed a trajectory-type method for globally optimizing multivariate quartic normal polynomials. Another strategy involves utilizing branch-and-bound algorithms, which partition the feasible region recursively and construct nonconvex quadratic or cubic lower bounds. Despite the advancements in these methods, they all face challenges associated with the curse of dimensionality. The computational complexity can grow exponentially with the number of variables of the polynomial, rendering certain methods impractical for large-scale problems.

Therefore, our work aims to develop more efficient algorithms specifically tailored for minimizing the m_3 model, taking into account its tensor structure and fourth-order regularization.

1.2 Motivation for Cubic Quartic Regularisation Method (CQR)

For notational simplicity³, we fix x_k and write $m_3(x_k, s)$ as

$$m_3(s) = f_0 + g^T s + \frac{1}{2}H[s]^2 + \frac{1}{6}T[s]^3 + \frac{\sigma}{4}\|s\|^4, \quad (2)$$

where $f_0 = f(x_k) = m_3(x_k, 0) \in \mathbb{R}$, $g = \nabla_x f(x_k) \in \mathbb{R}^n$, $H = \nabla_x^2 f(x_k) \in \mathbb{R}^{n \times n}$ and $T = \nabla_x^3 f(x_k) \in \mathbb{R}^{n \times n \times n}$. We also denote the fourth-order Taylor expansion⁴ of $m_3(s^{(i)} + s)$ at $s^{(i)}$ as

$$M(s^{(i)}, s) := f_i + g_i^T s + \frac{1}{2}H_i[s]^2 + \frac{1}{6}T_i[s]^3 + \frac{\sigma}{4}\|s\|^4, \quad (3)$$

where $f_i = m_3(s^{(i)}) \in \mathbb{R}$, $g_i = \nabla m_3(s^{(i)}) \in \mathbb{R}^n$, $H_i = \nabla^2 m_3(s^{(i)}) \in \mathbb{R}^{n \times n}$ and $T_i = \nabla^3 m_3(s^{(i)}) \in \mathbb{R}^{n \times n \times n}$ and ∇ denotes the derivative with respect to s . The fourth-order Taylor expansion is exact

³ $g^T s$ represents the usual Euclidean inner product of g and s , and $H[s]^2 = s^T H s$. $T[s_1][s_2] \dots [s_p]$ represents the tensor T applied sequentially to the vectors s_1, s_2, \dots, s_p , and similarly, $T[s]^p$ is the tensor T applied repeatedly to the vector s a total of p times.

⁴For all $s^{(i)}$, the Hessian H_i is a symmetric matrix. $T_i \in \mathbb{R}^{n \times n \times n}$ is a supersymmetric third-order tensor which means that the entries are invariant under any permutation of its indices. $T[s_1][s_2][s_3] = T[s_{\pi(1)}][s_{\pi(2)}][s_{\pi(3)}]$ where $\pi : \{1, 2, 3\} \rightarrow \{1, 2, 3\}$ is the permutation function.

since $m_3(s)$ is a fourth-degree multivariate polynomial. Therefore, we have $M(s^{(i)}, s) = m_3(s + s^{(i)})$, $\min_{s \in \mathbb{R}^n} m_3(s) = \min_{s \in \mathbb{R}^n} M(s^{(i)}, s)$, and $s^* := \operatorname{argmin}_{s \in \mathbb{R}^n} m_3(s) = s^{(i)} + \operatorname{argmin}_{s \in \mathbb{R}^n} M(s^{(i)}, s)$.

While globally minimizing the quartically regularized polynomial $M(s^{(i)}, s)$ is known to be NP-hard [24], we employ a quadratic model with a cubic degree term and quartic regularization to provide an approximation for $M(s^{(i)}, s)$. This model, which we refer to as the **Cubic Quartic Regularization (i.e., CQR) polynomial/model** can be expressed as follows

$$M_c(s^{(i)}, s) = f_i + g_i^T s + \frac{1}{2} H_i [s]^2 + \frac{\beta_i}{6} \|s\|_W^3 + \frac{\sigma_c^i}{4} \|s\|_W^4 \approx M(s^{(i)}, s), \quad (4)$$

where $\sigma_c^i > 0$, $\beta_i \in \mathbb{R}$, W is a symmetric, positive-definite matrix⁵. In the CQR polynomial, β_i typically provides insights into the tensor term $T_i[s]^3$, while σ_c is adjusted to control regularization and algorithmic progress. It is worth noting that our model accommodates negative values of β_i which is particularly useful as it yields information about the 'negative tensor directions' where $T_i[s]^3 < 0$. When $\beta_i = 0$ and $W = I_n$, $M_c(s^{(i)}, s)$ simplifies to the quadratic quartically-regularized (QQR) polynomials used in [14]. On the other hand, when $\beta_i > 0$ and $\sigma_c^i = 0$, $M_c(s^{(i)}, s)$ reduces to the quadratic model with cubic regularization polynomials, which is used in the ARC/AR2 algorithm [8; 17; 20; 26; 33]. However, note that for this paper, we require $\sigma_c^i > 0$ but allow $\beta_i \leq 0$.

The reason for choosing the CQR polynomial $M_c(s^{(i)}, s)$ to approximate $M(s^{(i)}, s)$ is that in this paper, we characterize the global minimizers of such CQR polynomials and devise a procedure to locate an approximate global minimizer of $M_c(s^{(i)}, s)$. Then, we minimize the CQR polynomial $M_c(s^{(i)}, s)$ iteratively and find a sequence of $\{s^{(i)}\}_{i \geq 0}$ such that $s^{(i)}$ converges to a second-order local minimizer of $M(s^{(i)}, s)$ (or equivalently m_3). We refer to this iterative minimization method as **the CQR algorithmic framework/method**. The updates for the CQR method are characterised by the following iterations

$$s_c^{(i)} = \operatorname{argmin}_{s \in \mathbb{R}^n} M_c(s^{(i)}, s), \quad s^{(i+1)} = s^{(i)} + s_c^{(i)}, \quad i := i + 1$$

where β_i, σ_c^i are adjusted adaptively in each iteration.

The paper presents the following key contributions:

- We develop necessary and sufficient optimality conditions for the global minimizers of $M_c(s^{(i)}, s)$. These conditions are general and applicable to both convex and nonconvex M_c and for both $\beta_i \geq 0$ and $\beta_i \leq 0$. Leveraging these optimality conditions, we can transform the problem of locating a global minimizer of $M_c(s^{(i)}, s)$ into a problem of solving a univariate nonlinear equation coupled with a matrix system that is similar to the trust region and ARC secular equations (Theorem 8.2.8 [7]). This opens up opportunities for developing efficient algorithms for minimizing $M_c(s^{(i)}, s)$. In this paper, we present an algorithm that is based on Cholesky factorization and Newton's root finding.

In the literature, there are related works on cubic polynomial multivariate models. For instance, Martinez and Raydan [25; 26] investigate the problem of the separable cubic model, where the cubic power term is expressed as $\sum_{j=1}^n \beta_j s_j^3$, with s_j being the j th entry of $s \in \mathbb{R}^n$ and β_j being scalar constants. However, these studies are conducted within the framework of cubic regularization or trust region methods [8; 9; 18; 19]. They do not incorporate third-order terms

⁵The matrix norm is defined as $\|v\|_W := \sqrt{v^T W v}$.

of the Taylor series in the objective function or its cubic approximations. The minimization of quartic regularized polynomials with specific cubic terms represents a relatively new research area. As far as we are aware, there are no algorithms explicitly designed for minimizing a quadratic model with a cubic degree term and a quartic regularization term.

- We then show global convergence properties of CQR algorithmic variants, analyzing the quality of the approximation provided by $M_c(s^{(i)}, s)$ to $m_3(s)$. Our theoretical analysis shows that CQR exhibits at least the same complexity as ARC and, in specific cases, the CQR algorithm demonstrates improved convergence behaviour. Practical CQR variants are proposed, where particular attention is given to the tensor approximation terms. Preliminary numerical experiments with these CQR variants also indicate that they usually identify an approximate stationary point of m_3 with fewer iterations or evaluations compared to the ARC method.

The paper is structured as follows: In Section 2, we explore necessary and sufficient optimality conditions that hold at a global minimizer of $M_c(s^{(i)}, s)$ and present an efficient algorithm in minimizing the CQR polynomial. Section 3 contains the convergence proof and complexity analysis of the CQR method. In addition, Appendix B proves that the iterates of the CQR method are uniformly bounded, a technical theorem crucial for analyzing the convergence and complexity of the CQR method. Finally, we provide algorithmic implementations and numerical examples in Section 4. The conclusion can be found in Section 5.

2 Characterising the Global Optimality of the CQR Polynomial

In this section, we develop necessary and sufficient conditions that hold at the global minimizers of $M_c(s^{(i)}, s)$ in 4. We convert the problem of finding a global minimizer of $M_c(s^{(i)}, s)$ into a problem of solving a nonlinear eigenvalue problem, which we can then solve using root-finding techniques. For the sake of notational simplicity, in this section, we write $M_c(s^{(i)}, s)$ as $M_c(s)$,

$$M_c(s) = f_i + g_i^T s + \frac{1}{2} H_i [s]^2 + \frac{\beta}{6} \|s\|_W^3 + \frac{\sigma_c}{4} \|s\|_W^4, \quad (5)$$

where σ_c represents σ_c^i and β as β_i . The derivatives of $M_c(s)$ has the expression

$$\nabla M_c(s) = g_i + H_i s + \frac{\beta}{2} \|s\|_W (W s) + \sigma_c \|s\|_W^2 (W s), \quad (6)$$

$$\nabla^2 M_c(s) = H_i + \frac{\beta}{2} \left(W \|s\|_W + \frac{(W s)(W s)^T}{\|s\|_W} \right) + \sigma_c \left(W \|s\|_W^2 + 2(W s)(W s)^T \right) \quad (7)$$

where ∇ is the derivative with respect to s and the matrix $(W s)(W s)^T$ is a rank-one matrix.

The section is organized as follows: In Section 2.1, we present global necessary optimality conditions for the CQR Polynomial in (5). In Section 2.2, we provide global sufficient optimality conditions. Finally, employing these conditions, in Section 2.3, we introduce an algorithm for locating an approximate minimizer of the CQR polynomial using nonlinear root-finding techniques.

2.1 Necessary Optimality Conditions for the CQR Polynomial

Theorem 2.1 provides a necessary condition for the global minimizers of $M_c(s)$, and we prove this theorem using a methodology similar to that of Theorem 8.2.7 in [7].

Theorem 2.1. (Necessary optimality conditions) Let s_c be a global minimizer of $M_c(s)$ in (5) over \mathbb{R}^n and let

$$B(s_c) := H_i + \frac{\beta}{2}W\|s_c\|_W + \sigma_c W\|s_c\|_W^2. \quad (8)$$

Then, s_c satisfies the system of equations

$$B(s_c)s_c = -g_i \quad (9)$$

and

$$B(s_c) \succeq 0. \quad (10)$$

If $B(s_c)$ is positive definite, s_c is unique.

Proof. The first-order necessary local optimality conditions at s_c give $g_i + H_i s_c + \frac{\beta}{2}\|s_c\|_W(Ws_c) + \sigma_c\|s_c\|_W^2(Ws_c) = 0$ and hence that (9) holds. The second-order necessary optimality gives

$$w^T \left[H_i + \frac{\beta}{2} \left(W\|s_c\|_W + \frac{(Ws_c)(Ws_c)^T}{\|s_c\|_W} \right) + \sigma_c \left(W\|s_c\|_W^2 + 2(Ws_c)(Ws_c)^T \right) \right] w \geq 0 \quad (11)$$

for all vectors $w \in \mathbb{R}^n$. If $s_c = 0$, (11) is equivalent to H_i being positive semi-definite, which immediately gives the result in (10). Thus, we only need to consider $s_c \neq 0$. There are two cases to consider. Firstly, suppose that $w^T Ws_c = 0$. In this case, it immediately follows from (11) that

$$w^T \underbrace{\left[H_i + \frac{\beta}{2}\|s_c\|_W W + \sigma_c\|s_c\|_W^2 W \right]}_{=B(s_c)} w \geq 0 \text{ for all } w \text{ for which } w^T Ws_c = 0. \quad (12)$$

It thus remains to consider vectors w for which $w^T Ws_c \neq 0$. Since w and s_c are not orthogonal with respect to the W -norm, the line $s_c + \tilde{k}w$ intersects the ball of radius $\|s_c\|_W$ at two points, s_c and u_* and thus

$$\|s_c\|_W = \|u_*\|_W. \quad (13)$$

We set $w_* = u_* - s_c$, and note that w_* is parallel to w . Since s_c is a global minimizer, we immediately have that

$$\begin{aligned} 0 &\leq M_c(u_*) - M_c(s_c) \\ &= g_i^T(u_* - s_c) + \frac{1}{2}u_*^T H_i u_* - \frac{1}{2}s_c^T H_i s_c + \frac{\beta}{6}(\|u_*\|_W^3 - \|s_c\|_W^3) + \frac{\sigma_c}{4}(\|u_*\|_W^4 - \|s_c\|_W^4) \\ &= g_i^T(u_* - s_c) + \frac{1}{2}u_*^T H_i u_* - \frac{1}{2}s_c^T H_i s_c \end{aligned}$$

where the last equality follows from (13). But (9) gives

$$(u_* - s_c)^T g_i = (s_c - u_*)^T H_i s_c + \frac{\beta}{2}\|s_c\|_W(s_c - u_*)^T Ws_c + \sigma_c\|s_c\|_W^2(s_c - u_*)^T Ws_c. \quad (14)$$

In addition, (13) gives

$$(s_c - u_*)^T Ws_c = \frac{1}{2}s_c^T Ws_c + \frac{1}{2}u_*^T Ws_c - u_*^T Ws_c = \frac{1}{2}w_*^T Ww_* = \frac{1}{2}\|w_*\|_W^2. \quad (15)$$

Thus we have

$$\begin{aligned} 0 &\leq M_c(u_*) - M_c(s_c) \\ &\stackrel{(14)}{=} (s_c - u_*)^T H_i s_c + \frac{\beta}{2}\|s_c\|_W(s_c - u_*)^T Ws_c + \sigma_c\|s_c\|_W^2(s_c - u_*)^T Ws_c + \frac{1}{2}u_*^T H_i u_* - \frac{1}{2}s_c^T H_i s_c \\ &\stackrel{(15)}{=} (s_c - u_*)^T H_i s_c + \frac{\beta}{4}\|s_c\|_W\|w_*\|_W^2 + \frac{\sigma_c}{2}\|s_c\|_W^2\|w_*\|_W^2 + \frac{1}{2}u_*^T H_i u_* - \frac{1}{2}s_c^T H_i s_c \\ &= \frac{1}{2}w_*^T H_i w_* + \frac{\beta}{4}\|s_c\|_W\|w_*\|_W^2 + \frac{\sigma_c}{2}\|s_c\|_W^2\|w_*\|_W^2 = \frac{1}{2}w_*^T \left[H_i + \frac{\beta}{2}\|s_c\|_W + \sigma_c\|s_c\|_W^2 \right] w_*. \end{aligned}$$

We deduce that

$$w^T \left[H_i + \frac{\beta}{2} \|s_c\|_W W + \sigma_c \|s_c\|_W^2 W \right] w \geq 0 \text{ for all } w \text{ for which } w^T W s_c \neq 0. \quad (16)$$

Hence, (12) and (16) together show that $H_i + \frac{\beta}{2} \|s_c\|_W W + \sigma_c \|s_c\|_W^2 W \succeq 0$. The uniqueness of s_c when $H_i + \frac{\beta}{2} \|s_c\|_W W + \sigma_c \|s_c\|_W^2 W$ is positive definite follows immediately from (9). \square

2.2 Sufficient Optimality Conditions for the CQR Polynomial

In this section, we derive sufficient optimality conditions using two approaches. Specifically, in Section 2.2.1, we establish a sufficient optimality condition inspired by Nocedal and Wright [34, Thm 4.1], while in Section 2.2.2, inspired by Cartis et al [7, Sec 8.2.1], we deduce another set of sufficient optimality conditions. Each approach corresponds to different cases of sufficiency. Finally, in Section 2.2.3, we integrate both proofs to provide an overall sufficient theorem (Theorem 2.6) that can be applied to all CQR polynomials.

2.2.1 Sufficient Optimality Conditions using Quadratic Forms Reformulations

In this section, we investigate sufficient conditions that hold at a global minimizer of $M_c(s)$, following a methodology inspired by Nocedal and Wright [34, Thm 4.1].

Theorem 2.2. (Sufficient optimality conditions using quadratic forms reformulations) *Let $B(s_c)$ be defined as in (8). Then, s_c is the global minimizer of $M_c(s)$ in (5) over \mathbb{R}^n if the following conditions are satisfied:*

1. g is in the range of $B(s_c)$, such that

$$B(s_c)s_c = \left(H_i + \frac{\beta}{2} W \|s_c\|_W I_n + \sigma_c W \|s_c\|_W^2 I_n \right) s_c = -g_i. \quad (17)$$

2. $B(s_c)$ is positive semidefinite, such that

$$B(s_c) := H_i + \frac{\beta}{2} W \|s_c\|_W + \sigma_c W \|s_c\|_W^2 \succeq 0. \quad (18)$$

3. β satisfies

$$\beta \geq -3\sigma_c \|s_c\|_W, \quad \text{or equivalently} \quad \|s_c\|_W \geq -\frac{\beta}{3\sigma_c}. \quad (19)$$

The global minimizer is unique if $B(s_c)$ is positive definite or $\beta > -3\sigma_c \|s_c\|_W$.

Proof. We assume wlog $f_i = 0$. For all vectors $w \in \mathbb{R}^n$, we have

$$\begin{aligned} M_c(s_c + w) &= g_i^T(s_c + w) + \frac{1}{2} H_i [s_c + w]^2 + \frac{\beta}{6} \|s_c + w\|_W^3 + \frac{\sigma_c}{4} \|s_c + w\|_W^4, \\ &= \underbrace{g_i^T(s_c + w) + \frac{1}{2} B(s_c) [s_c + w]^2 - \frac{\beta}{12} \|s_c\|_W^3 - \frac{\sigma_c}{4} \|s_c\|_W^4}_{\mathcal{F}_1} \\ &\quad - \underbrace{\frac{1}{2} \left[\frac{\beta}{2} \|s_c\|_W + \sigma_c \|s_c\|_W^2 \right] \|s_c + w\|_W^2 + \frac{\beta}{6} \|s_c + w\|_W^3 + \frac{\sigma_c}{4} \|s_c + w\|_W^4 + \frac{\beta}{12} \|s_c\|_W^3 + \frac{\sigma_c}{4} \|s_c\|_W^4}_{\mathcal{F}_2}. \end{aligned}$$

After rearranging,

$$\mathcal{F}_1 = \underbrace{\left[g_i^T s_c + \frac{1}{2} B(s_c)[s_c]^2 - \frac{\beta}{12} \|s_c\|_W^3 - \frac{\sigma_c}{4} \|s_c\|_W^2 \right]}_{=M_c(s_c)} + \underbrace{\left[g_i + B(s_c)s_c \right]}_{=0 \text{ by (17)}}^T w + \underbrace{\frac{1}{2} B(s_c)[w]^2}_{\geq 0 \text{ by (18)}}.$$

Therefore, we deduce that $\mathcal{F}_1 \geq M_c(s_c)$. Also, if $B(s_c)$ is positive definite, then, $\mathcal{F}_1 > M_c(s_c)$ for all $w \in \mathbb{R}^n$ with equality only at $w = 0$.

On the other hand, we denote $E = \|s_c\|_W$ and $F = \|s_c + w\|_W$, clearly $E \geq 0$ and $F \geq 0$. We can simplify and rearrange \mathcal{F}_2 as

$$\mathcal{F}_2 = \frac{1}{2}(E - F)^2 \left[\frac{\beta}{6}(E + 2F) + \frac{\sigma_c}{2}(E + F)^2 \right]. \quad (20)$$

Clearly, when $\beta \geq 0$, we have $\mathcal{F}_2 \geq 0$. Else, when $\beta \leq 0$, we let $\tilde{f}(F) := \frac{(E+F)^2}{(E+2F)}$ for $F \geq 0$; then $F_* := \operatorname{argmin}_{F \geq 0} \tilde{f}(F) = 0$ and $\tilde{f}(F_*) = E$. This implies that E is the best lower bound for $\tilde{f}(F)$ with $F \geq 0$. Together with condition (19), we have $0 \geq \beta \geq -3\sigma_c E \geq -3\sigma_c \frac{(E+F)^2}{(E+2F)}$. This immediately gives $\frac{\beta}{6}(E + 2F) + \frac{\sigma_c}{2}(E + F)^2 \geq 0$ and, consequently, $\mathcal{F}_2 \geq 0$. Note that if $\beta > -3\sigma_c \|s_c\|_W$, equality is attained only at $w = 0$.

Combining $\mathcal{F}_1 \geq 0$ and $\mathcal{F}_2 \geq 0$, we have $M_c(s_c + w) \geq M_c(s_c)$ for all $w \in \mathbb{R}^n$ and s_c is a global minimizer of M_c . If $B(s_c)$ is positive definite or $\beta > -3\sigma_c \|s_c\|_W$, we have $M_c(s_c + w) > M_c(s_c)$ for all $w \in \mathbb{R}^n / \{0\}$. □

Remark 2.1. (Discrepancy between sufficient and necessary conditions) *The sufficiency conditions (17)–(18) coincide with the necessary conditions (9)–(10). The distinction between sufficiency and necessity arises from the inclusion of (19), which imposes certain constraints on the choice of β . Namely, β should not be selected to have an excessively negative value.*

Remark 2.2. (Reduction to a cubically regularized quadratic polynomial) *Theorem 2.2 can be considered a generalization of sufficient conditions for the minimization of a cubically regularized quadratic polynomial [8; 33]. If $\sigma_c = 0$ and $\beta = 2\sigma_q > 0$, we recover the sufficient condition for the cubically regularized quadratic polynomial,*

$$M_q(s) = f_i + g_i^T s + \frac{1}{2} H_i [s]^2 + \frac{\sigma_q}{3} \|s\|_W^3.$$

The sufficiency condition (19) is naturally satisfied since $\beta > 0$. The sufficiency conditions (17) and (18) for the CQR polynomial reduce to the sufficiency conditions of the cubic regularized polynomial in [7, Thm 8.2.8].

2.2.2 Sufficient Optimality Conditions using a Secular Equation Approach

Theorem 2.3. (Sufficient optimality conditions using a secular equation approach) *Assume that H_i and β satisfy any one of the following cases,*

- **Case 1:** H_i is indefinite.
- **Case 2:** H_i is positive definite and $\beta \geq 0$.
- **Case 3:** H_i is positive definite, $-4\sqrt{\sigma_c \lambda_1} < \beta \leq 0$, and $\| [H_i - \frac{\beta^2}{16\sigma_c} W]^{-1} g \|_W \leq -\frac{\beta}{4\sigma_c}$ where λ_1 is the leftmost eigenvalue of the pencil $(H_i; W)$.

Let $s_c \in \mathbb{R}^n$ satisfy (9)–(10). Then, s_c is a global minimizer of $M_c(s)$ in (5) over \mathbb{R}^n .

Theorem 2.3 shares some similarities with Theorem 2.2. In particular, when $\beta \geq 0$, both proofs indicate that conditions (9)–(10) represent the necessary and sufficient condition for global optimality of s_c for M_c . When $\beta < 0$, (19) in Theorem 2.2 establishes the relationship between β and $\|s_c\|_W$ required to satisfy the sufficient optimality conditions. On the other hand, Case 3 in Theorem 2.3 provides the relationship between β and the eigenvalues of H_i to identify the global minimizer before computing $\|s_c\|_W$. A combined result of the two sufficiency theorems can be found in Section 2.2.3. In this subsection, our focus is on proving Theorem 2.3.

To prove Theorem 2.3, we first need to introduce the **secular equation**. To satisfy the conditions (9)–(10), we seek a vector $s(\lambda)$ which satisfies the system.

Secular Equation

$$B(s_c)s(\lambda) = (H_i + \lambda W)s(\lambda) = -g_i, \quad (21)$$

$$B(s_c) = H_i + \lambda W \succeq 0, \quad (22)$$

$$\lambda = \frac{\beta}{2}\|s(\lambda)\|_W + \sigma_c\|s(\lambda)\|_W^2. \quad (23)$$

where $B(s_c)$ is defined in (8).

To rearrange (22), let $\lambda_1 \leq \lambda_2 \leq \dots \leq \lambda_n$ be the eigenvalues of the pencil $(H_i; W)$ and let u_1, u_2, \dots, u_n be the corresponding generalised eigenvectors⁶ where each $u_i \in \mathbb{R}^n$. Then,

$$H_i U = W U D, \text{ where } U^T W U = I_n, \quad (24)$$

where $D \in \mathbb{R}^{n \times n}$ is the diagonal matrix with entries λ_i for $1 \leq i \leq n$, and $U \in \mathbb{R}^{n \times n}$ is the matrix whose columns are the u_i vectors for $1 \leq i \leq n$. Define $g_u := U^T g_i$ and $s_u(\lambda) = U^T W s(\lambda)$. From this, we may deduce that $s(\lambda) = U s_u(\lambda)$ and $g = W U g_u$ using (24). It then follows from (22) that

$$(H_i + \lambda W)s(\lambda) = (H_i + \lambda W)U s_u(\lambda) \stackrel{(24)}{=} W U (D + \lambda I) s_u(\lambda) = -g_i = -W U g_u.$$

Since W and U are nonsingular, therefore $s_u(\lambda) := (D + \lambda I)^{-1} g_u$. For $\lambda \neq -\lambda_i$ for any $1 \leq i \leq n$,

$$\Psi(\lambda) := \|s(\lambda)\|_W^2 = \|s_u\|_2^2 = \|(D + \lambda I)^{-1} U^T g_i\|^2 = \sum_{i=1}^n \frac{\gamma_i^2}{(\lambda + \lambda_i)^2} \quad (25)$$

where γ_i is the i th component of $U^T g_i$.

We also rearrange (23) to a nonlinear function of λ , such that

$$k_{\pm}(\lambda) := \frac{1}{4\sigma_c}(-\beta \pm \sqrt{\beta^2 + 16\lambda\sigma_c}) = \|s(\lambda)\|_W. \quad (26)$$

We say (26) is well defined if $k_{\pm}(\lambda) = \|s(\lambda)\|_W \geq 0$. Using (25) and (26), we give the nonlinear equations that need to be satisfied for λ .

⁶More details can be found in Appendix A.5 of [7].

Nonlinear Equations for λ

Let $\psi(\lambda) = \sqrt{\Psi(\lambda)}$, where $\Psi(\lambda)$ is defined in (25). Then, solving the secular equations (21)–(23) is equivalent to finding roots that satisfy

$$\psi(\lambda) = k_{\pm}(\lambda) = \frac{1}{4\sigma_c}(-\beta \pm \sqrt{\beta^2 + 16\lambda\sigma_c}) \quad \text{for } \lambda \geq -\lambda_1. \quad (27)$$

where λ_1 be the leftmost eigenvalue of the pencil $(H_i; W)$.

The sufficiency implication states that if we can prove the existence of a solution λ^* to (27), then it follows that the solution to the system (21)–(23) exists.

- If $H_i + \lambda^*W \succ 0$, (21) yields a unique s_c , indicating a unique global minimizer for $M_c(s)$.
- The hard case, similar to the trust-region subproblem [7, Sec 8.3.1], may occur when $\tau_1 := u_1^T g_i = 0$, leading to non-unique global minimizers for $M_c(s)$.

Case-by-case proof: global minimizer of $M_c(s)$ for $\tau_1 = u_1^T g_i \neq 0$.

We start with the standard cases when g_i is not orthogonal to the first generalised eigenvector of the pencil $(H_i; W)$ (i.e., $\tau_1 \neq 0$). We prove that, in these cases, there exist λ^* satisfying (27), and $H_i + \lambda^*W$ is positive definite. Thus, $M_c(s)$ has a unique global minimizer. To aid the proof, we define point \mathcal{A} as the intersection point for k_+ and k_- which has the coordinate $(\lambda_A, s_A) := (-\frac{\beta^2}{16\sigma_c}, -\frac{\beta}{4\sigma_c})$.

Case 1: If H_i is indefinite and $\tau_1 \neq 0$, we seek a solution satisfying $\lambda > -\lambda_1 \geq 0$. As illustrated by the right two plots in Figure 1, for all $\beta \in \mathbb{R}$ and $\lambda > -\lambda_1 \geq 0$, only $k_+(\lambda)$ is well defined (i.e. $k_+(\lambda) \geq 0$). Since $\psi(\lambda) = \sqrt{\Psi(\lambda)}$ is monotonically decreasing with $\lim_{\lambda \rightarrow -\lambda_1} \psi(\lambda) \rightarrow \infty$ and $\lim_{\lambda \rightarrow \infty} \psi(\lambda) \rightarrow 0$ and $k_+(\lambda)$ is monotonically increasing with $k_+(-\lambda_1) \geq 0$, there is a unique solution λ^* in the $k_+(\lambda)$ trench of (27). Note that $\lambda^* > -\lambda_1$ and $H_i + \lambda^*W \succ 0$, ensuring the existence of a unique global minimizer.

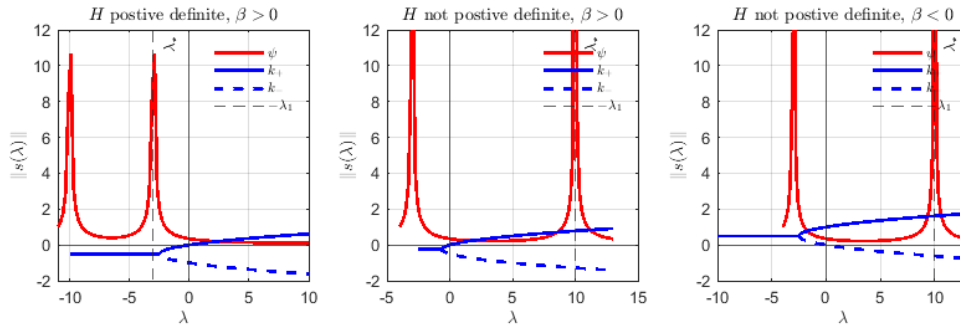


Figure 1: $\sigma_c = 10$, $W = I_2$, $g_i = [1, -1]^T$. **Left plot (Case 2):** $\beta = 20$, $H_i = [10, 0; 0, 3]$; **Mid plot (Case 1):** $\beta = 20$, $H_i = [-10, 0; 0, 3]$; **Right plot (Case 1):** $\beta = -20$, $H_i = [-10, 0; 0, 3]$.

Case 2: If $\beta \geq 0$, $H \succ 0$ and $\tau_1 \neq 0$, the intersection point $\mathcal{A} := (\lambda_A, s_A) = (-\frac{\beta^2}{16\sigma_c}, -\frac{\beta}{4\sigma_c})$ must be in the third quadrant and the only trench that is well defined is the $k_+(\lambda)$ for $\lambda > 0$ (An example illustrating this is given in the left plot in Figure 1). Moreover, $k_+(\lambda)$ is monotonically increasing for $\lambda > 0$ with $k_+(0) = 0$ and $\lim_{\lambda \rightarrow \infty} k_+(\lambda) \rightarrow \infty$. $\psi(\lambda)$ is monotonically decreasing with $\psi(0) > 0$ and $\lim_{\lambda \rightarrow \infty} \psi(\lambda) \rightarrow 0$. Thus, there is a unique solution λ^* lies in the $k_+(\lambda)$ trench for (27) with $\lambda^* > -\lambda_1$. The uniqueness of the global minimizer follows similarly to Case 1.

Case 3: If $\beta \leq 0$, $H \succ 0$, and $\tau_1 \neq 0$, as shown in Figure 2, (27) may have multiple solutions, so we need to impose extra conditions on β . The unique solution is in the k_- trench if point \mathcal{A} stays at the right of $\lambda = -\lambda_1$ and point \mathcal{A} is above ψ (the third plot of Figure 1). In other words,

$$\lambda_A = -\frac{\beta^2}{16\sigma_c} > -\lambda_1, \quad \text{and} \quad s_A = -\frac{\beta}{4\sigma_c} > \psi\left(-\frac{\beta^2}{16\sigma_c}\right).$$

Note that we have $\lambda^* \geq \lambda_A > -\lambda_1$, therefore $H_i + \lambda^*W \succ 0$, ensuring a unique global minimizer.

Lemma 2.4. (Case 3) Assume $H \succ 0$, and $\tau_1 \neq 0$, if $\beta \leq 0$ and satisfies $\frac{\beta^2}{16\sigma_c} < \lambda_1$ and $\psi(-\frac{\beta^2}{16\sigma_c}) = \|[H_i - \frac{\beta^2}{16\sigma_c}W]^{-1}g\|_W < -\frac{\beta}{4\sigma_c}$, then there exists a unique solution λ^* to (27) that lies in the $k_-(\lambda)$ trench.

Proof. Since $\beta \leq 0$, we have $\lambda_A = -\frac{\beta^2}{16\sigma_c} < 0$ and $s_A = \frac{\beta}{4\sigma_c} > 0$. Point \mathcal{A} which has coordinate $(\lambda_A, s_A) := (-\frac{\beta^2}{16\sigma_c}, -\frac{\beta}{4\sigma_c})$ is in the second quadrant. Since k_- is only well-defined for $\lambda > \lambda_A$, the range of interest for finding a solution is $\lambda \in (\lambda_A, 0)$. Both ψ and k_- are continuous and monotonic in the interval $(\lambda_A, 0)$, and $\psi(\lambda_A) \leq -\frac{\beta}{4\sigma_c} = k_-(\lambda_A)$ while $\psi(0) > 0 = k_-(0)$, while $\psi(0) > 0 = k_-(0)$, there must be a unique intersection between k_- and ψ within this interval. Lastly, we can clarify that the feasible root cannot occur in the k_+ trench. This is because k_+ is monotonically increasing and ψ is monotonically decreasing for all $\lambda > \lambda_A$ and $k_+(\lambda_A) = k_-(\lambda_A) > \psi(\lambda)$. \square

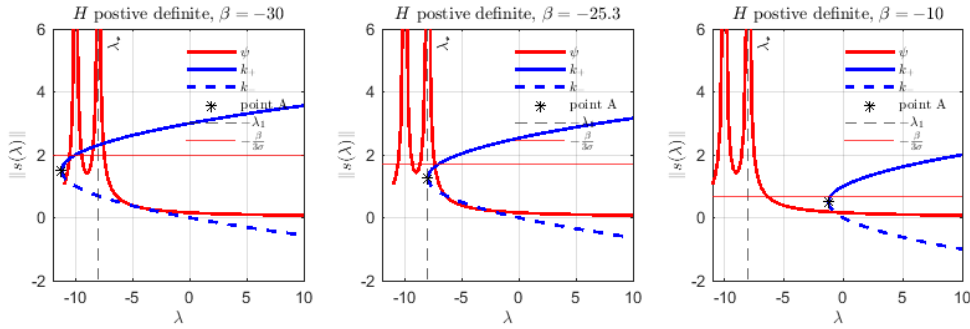


Figure 2: $\sigma_c = 5$, $W = I_2$, $g_i = [1, -1]^T$, $H_i = [10, 0; 0, 8]$. **Left plot (Case 4):** $\beta = -30$; **Mid plot (Case 5):** $\beta = -25.3$; **Right plot (Case 3):** $\beta = -10$.

Case-by-case proof: non-unique global minimizer of $M_c(s)$ for $\tau_1 = u_1^T g_i = 0$.

Now we consider the case where g_i is orthogonal to the generalised eigenvector of the pencil $(H_i; W)$ (i.e., $\tau_1 = u_1^T g_i = 0$). If $\tau_1 = 0$, we may have difficulties similar to the hard case of the trust-region subproblem [7, Sec 8.3.1].

Under these circumstances, (21) will be consistent if we set $\lambda = \lambda_s := -\lambda_1$, such that (21) becomes $(H + \lambda_s W)s_s = -g_i$. Thus, $H + \lambda_s W \succeq 0$, so (22) is satisfied. However, since $\lambda_1 = -\lambda_s$ is the leftmost eigenvalue of the pencil $(H_i; W)$, it follows that $(H_i + \lambda_s W)u_1 = 0$ for all u_1 corresponding to λ_1 and thus

$$g_i + (H_i + \lambda_s W)(s_s + k u_1) = 0 \tag{28}$$

for any scale $k \in \mathbb{R}$. Thus, in order to satisfy (23), we must additionally choose the scalar $k = k_s$ such that $\lambda_s = \frac{\beta}{2} \|s_s + k_s u_1\|_W + \sigma_c \|s_s + k_s u_1\|_W^2$. To obtain an exact solution in the hard case requires the generalised eigenvalue λ_1 , a corresponding eigenvector u_1 of H_i , and the ‘trajectory’ vector $s_s = \lim_{\lambda \rightarrow \lambda_s} s(\lambda) = -(H_i + \lambda_s W)^+ g$ where $(H_i + \lambda_s W)^+$ is the generalised inverse of $H_i + \lambda_s W$. We

summarize these results in the Theorem 2.5. More details and full proof can be found in [7, Corollary 8.3.1].

Theorem 2.5. *Any global minimizer of M_c may be expressed as*

$$s_c = s_s \text{ uniquely, if } \tau_1 \neq 0, \quad \text{or} \quad s_c = s_s + k_s u_1, \text{ if } \tau_1 = 0,$$

where $\tau_1 = u_1^T g_i$, $s_s = -(H_i + \lambda_s W)^+ g_i$ and $\lambda_s = \frac{\beta}{2} \|s_c\|_W + \sigma_c \|s_c\|_W^2 > -\lambda_1$, where k_s is one of the two roots of $\lambda_s = \frac{\beta}{2} \|s_s + k_s u_1\|_W + \sigma_c \|s_s + k_s u_1\|_W^2$.

2.2.3 General Sufficient Optimality Conditions for the Global Minimum of M_c

In this subsection, we integrate Theorem 2.2 and Theorem 2.3 to provide a general sufficient optimality result along with a graphical representation of the feasible values of β (Figure 3). The sufficient conditions in Theorem 2.3 correspond to Cases 1 to 3 in Theorem 2.6. The sufficiency conditions in Theorem 2.2 not only confirm the results of Theorem 2.3 but also extend the range of cases that we can address (see Case 4).

General Sufficient Optimality Conditions for the Global Minimum of M_c

Theorem 2.6. *Consider the CQR polynomial $M_c(s)$ in (5), let $s_c \in \mathbb{R}^n$ be a vector that satisfies (21), (22), and (27) with the corresponding trench selected as described in Case 1 to Case 5 below. Then, s_c is a global minimizer of $M_c(s)$ over \mathbb{R}^n .*

- **Case 1:** (From Theorem 2.2 and Theorem 2.3) H_i is indefinite, take k_+ trench in (27).
- **Case 2:** (From Theorem 2.2 and Theorem 2.3) H_i is positive definite and $\beta \geq 0$, take k_+ trench in (27).
- **Case 3:** (From Theorem 2.3) H_i is positive definite,

$$-4\sqrt{\sigma_c \lambda_1} \leq \beta \leq 0, \quad \text{and} \quad -\frac{\beta}{4\sigma_c} > \psi\left(-\frac{\beta^2}{16\sigma_c}\right) = \left\| \left(H_i - \frac{\beta^2}{16\sigma_c} W \right)^{-1} g \right\|_W, \quad (29)$$

take k_- trench in (27).

- **Case 4:** (From Theorem 2.2) H_i is positive definite, $\beta \leq -3\sqrt{2}\sqrt{\lambda_1\sigma_c} \approx -4.24\sqrt{\lambda_1\sigma_c}$, take k_+ trench in (27).
- **Case 5:** In the rest of the cases, namely, H_i is positive definite and $-3\sqrt{2}\sqrt{\lambda_1\sigma_c} \leq \beta \leq -4\sqrt{\lambda_1\sigma_c}$. Or H_i is positive definite,

$$-4\sqrt{\lambda_1\sigma_c} \leq \beta \leq 0 \quad \text{and} \quad -\frac{\beta}{4\sigma_c} < \psi\left(-\frac{\beta^2}{16\sigma_c}\right) = \left\| \left(H_i - \frac{\beta^2}{16\sigma_c} W \right)^{-1} g \right\|_W.$$

Up to three solutions satisfying (27) may exist. The solution that minimizes the function value of M_c corresponds to the global minimizer. A root, denoted by (λ_+, s_+) , within the k_+ trench exists, and this solution satisfies $M_c(s_+) < M_c(0)$.

Remark 2.3. *Cases 1, 2, and 3 follow from Theorem 2.3. Cases 1, 2, and 4 are derived from Theorem 2.2, and therefore, $\|s_c\|_W$ satisfies $\|s_c\|_W \geq -\frac{\beta}{3\sigma_c}$.*

Remark 2.4. All values of $\beta \in \mathbb{R}$ are addressed in Theorem 2.6. This indicates that by finding the root of (27) that satisfies (21) and (23), we can find a global minimizer of M_c for all $\beta \in \mathbb{R}$ and $\sigma_c > 0$. The intersection point of the k_+ and k_- trenches, denoted as $\mathcal{A} = (\lambda_A, s_A) = \left(-\frac{\beta^2}{16\sigma_c}, -\frac{\beta}{4\sigma_c}\right)$, corresponds to various cases outlined in Theorem 2.6. When H is indefinite, regardless of the location of point \mathcal{A} , we are in Case 1 (as shown in the left plot of Figure 3). If H is indefinite, when point \mathcal{A} falls within specific colored regions, it corresponds to the cases described in Theorem 2.6 (as shown in the right plot of Figure 3). As illustrated in Figure 3, Cases 1–4 encompass the majority of β values, while Case 5 covers the remaining situations. An example of Case 5 is presented in the second plot of Figure 2.

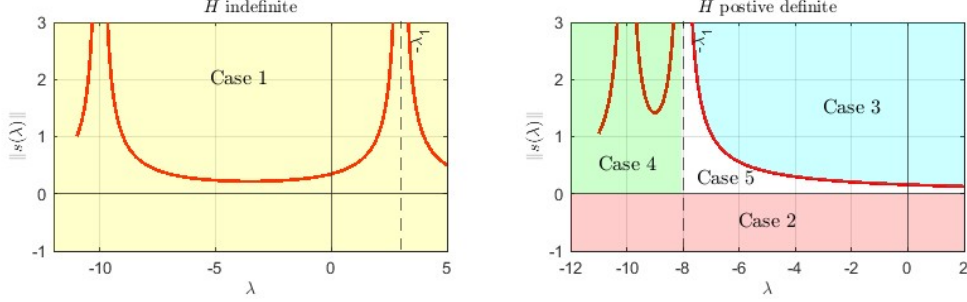


Figure 3: Illustration plot depicting the location of point \mathcal{A} corresponding to different cases outlined in Theorem 2.6. $\sigma_c = 5$, $W = I_2$, $g_i = [1, -1]^T$, $H_i = [10, 0; 0, -3]$ for the left plot and $H_i = [10, 0; 0, 8]$ for the right plot. The red curve represents $\psi(\lambda)$.

Proof. **Case 1 and Case 2:** follows from Theorem 2.2 and Theorem 2.3. According to Theorem 2.2, if $\beta \geq 0$, we can observe from (20) that $\mathcal{F}_2 > 0$, and consequently, $M_c(s + w) > M_c(s)$ for all $w \in \mathbb{R}^n$. The condition on β is naturally satisfied. According to Theorem 2.3, as discussed in the case-by-case analysis, there exists a unique root $\lambda^* > -\lambda_1$ in the $k_+(\lambda)$ for the nonlinear equation (27).

Case 3: follows from Theorem 2.3. This case is established using Theorem 2.3 and Lemma 2.4. It is worth noting that this case cannot be derived using Theorem 2.2. The reason is that any solution found in the k_- trench satisfies $\|s_c\|_W \leq s_A = -\frac{\beta}{4\sigma_c}$, which does not always meet the conditions of (19).

Case 4: follows from Theorem 2.2. Assuming $\beta \leq 0$, $H \succ 0$, and $\tau_1 \neq 0$, the sufficiency conditions provided in Theorem 2.2 offer an alternative approach to characterise the global minimizer. If point \mathcal{A} is positioned to the left of $\lambda = -\lambda_1$ and the value of k_+ at $\lambda = -\lambda$ satisfy $k_+(-\lambda) \geq -\frac{\beta}{3\sigma_c}$ (as depicted in the first plot of Figure 2), then there exists a solution that satisfies the sufficient condition in Theorem 2.2. This solution lies within the k_+ trench and represents the global minimizer of M_c . In other words, to meet the sufficient condition in Theorem 2.2, the following conditions are required:

$$\lambda_A = -\frac{\beta^2}{16\sigma_c} \leq -\lambda_1, \quad \text{and} \quad k_+(-\lambda_1) = \frac{1}{4\sigma_c}(-\beta + \sqrt{\beta^2 - 16\lambda_1\sigma_c}) \geq -\frac{\beta}{3\sigma_c}.$$

This implies $\beta \leq -3\sqrt{2}\sqrt{\lambda_1\sigma_c}$.

Case 5: In the remaining cases, there may be up to three solutions satisfying (27) as depicted in the second plot of Figure 2. By the necessary optimality conditions, the solution that minimizes the function value of M_c corresponds to the global minimizer. As point \mathcal{A} either lies below the curve $\psi(\lambda)$

or to the left of $\lambda = -\lambda_1$, a root in the k_+ trench is always guaranteed. Let (λ_+, s_+) be the root in the k_+ trench satisfying (27) and consequently satisfying (21)–(23). We deduce that

$$\begin{aligned} M_c(0) - M_c(s_+) &= -g_i^T s_+ - \frac{1}{2} H_i [s_+]^2 - \frac{\beta}{6} \|s_+\|^3 - \frac{\sigma_c}{4} \|s_+\|^4 \stackrel{(21)}{=} \frac{1}{2} H_i [s_+]^2 + \frac{\beta}{3} \|s_+\|^3 + \frac{3\sigma_c}{4} \|s_+\|^4 \\ &\geq \|s_+\|^2 \left(\frac{1}{2} \lambda_1 + \frac{\beta}{3} \|s_+\| + \frac{3\sigma_c}{4} \|s_+\|^2 \right) > 0. \end{aligned}$$

Since $\lambda_1 > 0$ and $-3\sqrt{2}\sqrt{\lambda_1\sigma_c} \leq \beta < 0$, the discriminant of the quadratic equation $q(\|s_+\|) := \frac{1}{2}\lambda_1 + \frac{\beta}{3}\|s_+\| + \frac{3\sigma_c}{4}\|s_+\|^2$ is negative, i.e., $\frac{\beta^2}{9} - \frac{3\lambda_1\sigma_c}{2} < 0$. This gives $M_c(0) - M_c(s_+) \geq 0$. \square

2.3 An Algorithm for Minimizing the CQR Polynomial

As suggested by Theorem 2.1 and Theorem 2.6, we have transformed the task of identifying a global minimizer of M_c into the problem of solving the nonlinear equations (27) for λ in the corresponding trench. To numerically determine the root of (27), we utilize the global optimality characterisations outlined in Sections 2.1 to 2.2. Additionally, we extend well-established Cholesky factorization-based root-finding techniques, as detailed in [7, Ch 8.2.3]. The primary objective of this subsection is to formulate an algorithm for locating the root of the univariate nonlinear equation. We opt to employ univariate Newton iteration to find the necessary root of (27). Further convergence analysis for the root-finding method is deferred to future work.

In practice, as suggested by [8, Sec 6.1], instead of solving (27), it may be preferable to solve

$$\phi_1(\lambda) := [\psi(\lambda)]^{-1} - [k_{\pm}(\lambda)]^{-1} = 0 \quad \text{for} \quad \lambda \geq \lambda_1 \quad (30)$$

where the choice between using k_+ trench or k_- trench is made on a case-by-case basis, as determined by Theorem 2.6. The updates for the Newton iteration are detailed in Lemma 2.7.

Lemma 2.7. *Suppose $g \neq 0$, the Newton iteration updates are*

$$\Delta\lambda^k = \frac{\phi_1(\lambda)}{\phi_1'(\lambda)} = \frac{\|s(\lambda)\|_W^{-1} - [k_{\pm}(\lambda)]^{-1}}{\|\omega(\lambda)\|_W^2 \|s(\lambda)\|_W^{-3} - [(k_{\pm}(\lambda))^{-1}]'}, \quad \lambda^{(k+1)} = \lambda^{(k)} + \Delta\lambda^k \quad (31)$$

where $\omega(\lambda)$ is given by $W^{-1}(H_i + \lambda W) = L(\lambda)L^T(\lambda)$ and $L(\lambda)\omega(\lambda) = s(\lambda)$. Also,

$$k_{\pm}^{-1}(\lambda) = \frac{2\sigma_c}{-\beta \pm \sqrt{\beta^2 + 4\lambda\sigma_c}}, \quad [(k_{\pm}(\lambda))^{-1}]' = \frac{\mp 4\sigma_c^2}{(-\beta \pm \sqrt{\beta^2 + 4\lambda\sigma_c})^2 (\beta^2 + 4\lambda\sigma_c)^{1/2}}.$$

Sketch of Proof. Based on [8, Lemma 6.1], we have given the Cholesky factorization $W^{-1}(H_i + \lambda W) = L(\lambda)L^T(\lambda)$, then

$$\Psi'(\lambda) = 2s(\lambda)^T W \nabla_{\lambda} s(\lambda) = -2\|\omega(\lambda)\|_W^2 \quad (32)$$

where $L(\lambda)L^T(\lambda)s(\lambda) = -Wg$ and $L(\lambda)\omega(\lambda) = s(\lambda)$. Consequently,

$$(\psi(\lambda)^{-1})' = (\Psi(\lambda)^{-1/2})' = -\frac{1}{2}\Psi(\lambda)^{-3/2}\Psi'(\lambda) = \|s(\lambda)\|_W^{-3}\|\omega(\lambda)\|_W^2. \quad (33)$$

Substituting (33) into the Newton updates $\Delta\lambda^k = \frac{\phi_1(\lambda)}{\phi_1'(\lambda)}$ gives the result. More details are in Appendix A and Lemma 7.3.1 in [16].

Numerical Set-up and Initialization for the Newton Step

In a similar manner to the techniques used to solve the trust region and ARC subproblems [7, Ch 8.2.3] [8, Sec 6.1], for the minimization of the CQR polynomial in (4), we employ Newton's method to solve the secular equation (30). As described in Theorem 2.6, the solution of the secular equation (30) falls into either Case 1, 2, 4, or 5, where it resides in the k_+ trench, or Case 3, where it lies within the k_- trench.

In practical implementation, we first search for a solution in the k_+ trench using the initialization in Remark 2.5. If no solution is found in the k_+ trench, we proceed to search for a solution in the k_- trench. Based on our numerical experiments in Section 4, we find that in approximately 90% of the iterations, the solution lies in the k_+ trench. The algorithm is detailed in Algorithm 1, and the initialization details are provided in Remark 2.5

Algorithm 1: Newton's method to Solve (30)

Initialization: Initialize the counter $k = 0$, $s^{(0)} = 0$ and $\lambda^{(0)}$ as in Remark 2.5. Set an accuracy level $\epsilon_N > 0$, usually $\epsilon_N = 10^{-8}$ smaller than the accuracy of the subproblem.

Initialize trench: Choose k_+ trench: $k_T(\cdot) := k_+(\cdot)$.

Input: f_i, g_i, H_i, β and $\sigma_c > 0$.

while $\|s^{(k)}\| - k_T(\lambda^{(k)}) > \epsilon$ **do**

if $H_i + \lambda^{(k)}I_n \succ 0$ **then**

 Cholesky factorize $(H_i + \lambda^{(k)}I_n) = LL^T$. Solve $LL^T s^{(k)} = -g_i$ and $L\omega^{(k)} = s^{(k)}$.

 Compute the Newton update step:

$$\Delta\lambda^k = \frac{\phi_1(\lambda^{(k)})}{\phi_1'(\lambda^{(k)})} = \frac{\|s^{(k)}\|_W^{-1} - [k_T(\lambda^{(k)})]^{-1}}{\|\omega^{(k)}\|_W^2 \|s^{(k)}\|_W^{-3} - [(k_T(\lambda^{(k)}))^{-1}]'}, \quad \lambda^{(k+1)} = \lambda^{(k)} + \Delta\lambda^k.$$

else

 Switch to k_- trench: $k_T(\cdot) = k_-$. Set $\lambda^{(0)} = 0$.

Initialization for the Newton Algorithm

Remark 2.5. In Cases 1, 2, 4, and 5, where the solution resides in the k_+ trench, we initialize $\lambda^{(0)}$ as follows:

- Case 1 and Case 2: If H_i is indefinite, we set $\lambda^{(0)} := \max\{-\lambda_1, 0\} + 10^{-6}$. This ensures $H + \lambda^{(0)}I \succ 0$.
- Case 4 and 5: If $H_i \succ 0$ and $\beta < 0$, we set $\lambda^{(0)} := \max\{-\lambda_1, \lambda_A\} + 10^{-6}$ where $\lambda_A = -\frac{\beta^2}{16\sigma_c}$ denotes the intersection point for k_+ and k_- . This initialization also ensures $H + \lambda^{(0)}I \succ 0$. This choice is motivated by the observation that, as illustrated in the two leftmost plots of Figure 2, the solution to the secular equation (30) consistently resides in the right side of $\lambda = -\lambda_{\min}[H]$ and $\lambda = \lambda_A$.

If no solution is found in the k_+ trench, it implies we are in Case 3. Consequently, we proceed to seek a solution within the k_- trench. In Case 3, where $H_i \succ 0$ and $\beta < 0$, as illustrated on the rightmost plot in Figure 2, the solution to the secular equation (30) is near $\lambda = 0$ and falls within the interval $[\lambda_A, 0]$. Therefore, we initialize $\lambda^{(0)} = 0$.

Remark 2.6. *Regardless of the case, we ensure that $H_i + \lambda^{(0)}I_n$ is positive definite, making the Cholesky factorization possible in the first iteration. While it is worth noting that this does not entirely avoid the hard case, as it is only the first iteration, this is a measure we take to ensure that we do not start the algorithm with an indefinite $H_i + \lambda^{(0)}I_n$. Throughout the iterations of Algorithm 1, in all the numerical examples we examined, the positive definiteness of $H_i + \lambda^{(k)}I_n$ is preserved, and we did not encounter the hard case. The Cholesky factorization also remains valid in the cases we tested. However, note that Algorithm 1 is a preliminary implementation of Newton root-finding for the nonlinear equation (27). Addressing and implementing the hard case, as well as the convergence analysis of Algorithm 1, is dedicated to future work.*

Remark 2.7. *Theorem 2.1 and Theorem 2.6 give a global optimality characterization for the CQR polynomial in (4). However, in Case 5 of Theorem 2.6, up to three solutions may exist. Then, since we are using Newton’s method, depending upon the initialization, Algorithm 1 may converge to a root in k_+ which corresponds to a local minimizer of M_c . To locate the global minimizer in Case 5, one needs to locate all the roots in the k_+ and k_- trench (there are at most three roots) and evaluate the value of M_c at these roots. The roots that give the lowest function value of M_c will correspond to global minimizers of M_c . We defer the implementation of this additional root-finding procedure to future algorithmic developments. Numerically, in all the cases that we tested, the algorithm converges to a global minimizer in Cases 1–4 and converges to a local minimizer $s^{(K)}$, with a decrease in M_c value in Case 5, such that $M_c(s^{(K)}) < M_c(s^{(0)})$.*

Our current approach here, for solving the system (21)–(23) and (27), uses Cholesky factorization and Newton’s method to address the secular equation (27), and is just one of many possibilities. Similarly to existing approaches for trust region and regularization subproblems ([8, Ch. 6] and [13, Ch. 8, 10]), scalable iterative algorithms could be designed here, based on Krylov methods, eigenvalue formulations, or subspace optimization. While we recognize the potential of these tools for solving (21)–(23) and finding the global minimum of the CQR polynomial, our primary focus in this paper is on using the CQR polynomial to minimize the m_3 subproblem. As a result, we defer a detailed analysis of these alternative approaches to future work.

3 The CQR Algorithmic Framework for Minimizing m_3

The CQR algorithm minimizes the AR3 subproblem (i.e., m_3 as defined in (2)) by globally minimizing a sequence of potentially nonconvex CQR polynomials (i.e., quadratic models with cubic term and quartic regularization)⁷. Additionally, the CQR algorithmic framework is tensor-free in the sense that we do not require the entries of T to be stored; we only need vector and matrix products with the tensor T (such as $T[s]$ or $T[s]^2$). We define the norms of the derivatives as $\|g\| := \sqrt{g^T g}$, $\|H\| := \max_i |\lambda_i(H)|$, and $\|T\| = \max_{\|u_1\|=\|u_2\|=\|u_3\|=1} |T[u_1][u_2][u_3]| < \infty$. In this section and the rest of the paper, when constructing the CQR model M_c in (4), we choose $W = I_n$. Algorithm 2 outlines the framework of the CQR algorithm.

Remark 3.1. (*Purpose of β_i*) *The purpose of β_i is to provide a scalar approximation of the third-order information $\frac{T[s]^3}{\|s\|^3}$. For a given tensor $T \in \mathbb{R}^{n \times n \times n}$, $\frac{T[s]^3}{\|s\|^3}$ is bounded. Also, the term $\frac{T[s]^3}{\|s\|^3}$ can be*

⁷For a fixed subproblem in (2), x_k is fixed, and we have access to the coefficients for the subproblem; namely, $f_0 = f(x_k)$, $g = \nabla_x f(x_k)$, $H = \nabla_x^2 f(x_k)$, $T = \nabla_x^3 f(x_k)$, and $\sigma > 0$.

Algorithm 2: CQR Algorithmic Framework with Adaptive Regularization

Initialization: Set $s^{(0)} = \mathbf{0} \in \mathbb{R}^n$ and $i = 0$. An initial regularization parameter $d_0 = 1$, constants $\eta_1 > \eta > 0$, $\gamma > 1 > \gamma_2 > 0$.

Input: $f_0 := m_3(s^{(0)})$, $g_0 := \nabla m_3(s^{(0)})$, $H_0 := \nabla^2 m_3(s^{(0)})$, $\sigma > 0$ is the given regularization parameter in m_3 as defined in (2); an accuracy level $\epsilon > 0$.

Step 1: Test for termination. If $\|g_i\| = \|\nabla m_3(s^{(i)})\| \leq \epsilon$, terminate with the ϵ -approximate first-order minimizer $s_\epsilon = s^{(i)}$.

Step 2: Step computation. Compute β_i to give a scalar representation of the (local) tensor information in m_3^a . Set

$$M_c(s^{(i)}, s) := f_i + g_i s + \frac{1}{2} H_i [s]^2 + \frac{1}{6} \beta_i \|s\|^3 + \underbrace{\left(\frac{\sigma}{4} + d_i \right)}_{:= \sigma_c^i} \|s\|^4. \quad (\text{CQR Model})$$

Compute $s_c^{(i)} = \operatorname{argmin}_{s \in \mathbb{R}^n} M_c(s^{(i)}, s)$ (see Remark 3.3).

Step 3: Acceptance of trial point. Compute $m_3(s^{(i)} + s_c^{(i)})$ and define

$$\rho_i = \frac{m_3(s^{(i)}) - m_3(s^{(i)} + s_c^{(i)})}{m_3(s^{(i)}) - M_c(s^{(i)}, s_c^{(i)})}. \quad (\text{Ratio Test})$$

Step 4: Regularization Parameter Update.

- If $\rho_i \geq \eta_1$ (*very successful step*): Set $s^{(i+1)} = s^{(i)} + s_c^{(i)}$, $d_{i+1} = \gamma_2 d_i$, update β_{i+1} (details in Section 4), and compute g_{i+1} .
- If $\eta \leq \rho_i \leq \eta_1$ (*successful step*): Set $s^{(i+1)} = s^{(i)} + s_c^{(i)}$, $d_{i+1} = d_i$, update β_{i+1} , and compute g_{i+1} .
- If $\rho_i \leq \eta$, (*unsuccessful step*) $s^{(i+1)} = s^{(i)}$, increase $d_{i+1} = \gamma d_i$, $\beta_{i+1} = \beta_i$.

Increment i by one and go to Step 1.

^aDetails about selecting β_i can be found in Algorithm 4 in Section 4.

either positive or negative. Therefore, we allow β_i to take both positive and negative values. We also assume that β_i is bounded for all iterations, as outlined in Assumption 1. The bound for β_i is used for the convergence of the CQR algorithm, ensuring optimal complexity and practical numerical implementation. This bound can be easily applied in practice, such as by setting $B = \max_{1 \leq l, j, k \leq n} |T[l, j, k]|$ in the practical CQR algorithm (Algorithm 4 in Section 4), to prevent $|\beta_i|$ from becoming excessively large. More details about the computation of β_i are discussed in Section 4.

Assumption 1. For every iteration, i , β_i is uniformly bounded, such that $|\beta_i| \leq B$.

Remark 3.2. (Purpose of d_i) d_i is an adaptive regularization parameter; $d_i \geq 0$ ensures that M_c remains bounded from below. In some iterations, if β_i is positive, then $\beta_i \|s\|^3$ can serve as a regularization term for the M_c model, potentially superseding the role of the quartic regularization term $d_i \|s\|^4$. Thus, in these iterations, we have more flexibility in choosing d_i (i.e., we can set $d_i = 0$).

Remark 3.3. (Minimization of M_c) In Algorithm 2, we assume that we find a global minimizer of M_c , such that $s_c^{(i)} = \operatorname{argmin}_{s \in \mathbb{R}^n} M_c(s^{(i)}, s)$. For optimal complexity analysis, we focus on a variant of the CQR algorithmic framework (Section 3.1). While our proof in Section 3.1 (in particular Lemma 3.2) assumes exact minimization of $\nabla M_c(s^{(i)}, s_c) = 0$, similar bounds can be derived when considering approximate minimization of M_c with a step-termination condition, such as $\|\nabla M_c(s^{(i)}, s_c)\| \leq \Theta \|s_c\|^3$ for some $\Theta \in (0, 1)$. Such step-termination conditions are also used in [12], with alternative variants available [8].

It is worth noting that the CQR method can be applied directly to the minimization of an objective function (not just m_3). If the objective function satisfies suitable Lipschitz conditions and is bounded below, then the CQR method can also be used for local minimization of a potentially nonconvex objective function. However, our interest here is not to create a general method for optimizing f , instead, we focus on efficiently minimizing m_3 .

This section is organized as follows: In Section 3.1, we introduce a variant of the CQR algorithmic framework and establish its convergence guarantee. We demonstrate that this variant requires at most $O(\epsilon^{-3/2})$ function and derivative evaluations to compute an approximate first-order critical point of m_3 that satisfies $\|g_i\| \leq \epsilon$. This bound is at least as good as that of the ARC algorithm for minimizing m_3 . In Section 3.2, we explore specific instances of m_3 where CQR algorithm exhibits improved convergence behavior.

3.1 Convergence and Complexity of a CQR Algorithmic Variant

Algorithm 3 is a variant of the CQR algorithmic framework (Algorithm 2) for which we prove an optimal worst-case complexity bound.

In this variant, we introduce a new constant, $\alpha \in [0, \frac{1}{2}]$, to further control the step length s_c . Due to this additional parameter and the step size control, we need to consider two additional cases in which we reject the step and increase regularization. The first case occurs when $-B \leq \beta_i \leq -4\alpha$, and σ_c falls within the narrow region of $[\frac{1}{6}, \frac{2}{3}] (-\beta_i + \alpha) |s_c^{(i)}|^{-1}$. The second case arises when β_i is in the narrow range of $[-4\alpha, \alpha]$, and $\sigma_c^i \geq \frac{2}{3} (-\beta_i + \alpha) |s_c^{(i)}|^{-1}$. For the remaining cases where β_i and σ_c^i do not fit into these two scenarios, the ratio test defined in (Ratio Test) with an outcome of $\rho_i \geq \eta$ is sufficient to determine the success of the step.

Algorithm 3: A CQR Variant of Algorithm 2

Fix a constant $\alpha \in (0, \frac{1}{2})$. Initialize and proceed through Steps 1 to 3 following the same procedure as outlined in the CQR algorithmic framework (Algorithm 2). In Step 4, we utilize the following rule for updating the regularization parameter, β_{i+1} and $s^{(i+1)}$.

if $\|\nabla m_3(s^{(i)} + s_c^{(i)})\| \leq \epsilon$ **then**

└ **Terminate** with an ϵ -approximate first-order minimizer s_ϵ of $m_3(s^{(i)} + s_c^{(i)})$.

else

└ **if** $\rho_i \geq \eta$ and $\beta_i \in [\alpha, B]$ **then**

└ *Successful Step:* $s^{(i+1)} := s^{(i)} + s_c^{(i)}$, update $0 \leq d_{i+1} \leq d_i$, update β_{i+1} (details in Section 4), compute g_{i+1} .

└ **else if** $\rho_i \geq \eta$ and $\beta_i \in [-B, -4\alpha]$ and $\sigma_c^i \notin [\frac{1}{6}, \frac{2}{3}] (-\beta_i + \alpha) \|s_c^{(i)}\|^{-1}$ **then**

└ *Successful Step:* $s^{(i+1)} := s^{(i)} + s_c^{(i)}$, update $0 \leq d_{i+1} \leq d_i$, update β_{i+1} , compute g_{i+1} .

└ **else if** $\rho_i \geq \eta$ and $\beta_i \in [-4\alpha, \alpha]$ and

$$\sigma_c^i \geq \frac{2}{3} (-\beta_i + \alpha) \|s_c^{(i)}\|^{-1} \tag{34}$$

└ **then**

└ *Successful Step:* $s^{(i+1)} := s^{(i)} + s_c^{(i)}$, update $0 \leq d_{i+1} \leq d_i$, update β_{i+1} , compute g_{i+1} .

└ **else**

└ *Unsuccessful Step:* $s^{(i+1)} := s^{(i)}$, $\beta_{i+1} := \beta_i$ and increase $d_{i+1} := \gamma \max\{1, d_i\}$.

It is also important to note that whenever we satisfy $\rho_i \geq \eta$ as illustrated in the CQR algorithmic framework (Algorithm 2), even without the requirement for $\sigma_c^{(i)}$ in Algorithm 3, we are guaranteed to have a decrease in values of m_3 at each successful iteration,

$$m_3(s^{(i)}) - m_3(s^{(i+1)}) \geq \eta \left[m_3(s^{(i)}) - M_c(s^{(i)}, s_c^{(i)}) \right] > 0$$

where $\eta \in (0, 1]$. In essence, the CQR algorithmic framework (Algorithm 2) ensures convergence to an approximate local minimum of m_3 that adheres to first-order optimality conditions. But our aim in this section is to establish a global rate of complexity bound, hence the need to introduce an additional requirement involving α .

To establish convergence and determine the complexity bound for Algorithm 3, we adopt a framework similar to the convergence proof for AR1 as presented in [7, Sec 2.4.1]. The proof is structured as follows:

1. **Groundwork:** We establish upper and lower bounds for the step size (Theorem 3.1 and Lemma 3.2) using an upper bound on the tensor term (Corollary 3.1).
2. **Decrease in the value of m_3 :** We prove that the CQR model constructed in successful steps of Algorithm 3 yields a decrease in the value of m_3 by at least $O(\epsilon^{-3/2})$, where ϵ represents the prescribed first-order optimality tolerances (Theorem 3.3 and Theorem 3.5).
3. **Bounded Iterations:** We establish that there is a limited number of unsuccessful iterations (Lemma 3.4 and Lemma 3.6).

Combining these results, we derive the complexity bound for Algorithm 3 (Lemma 3.7 and Theorem 3.8). Specifically, Algorithm 3 is guaranteed to find a first-order critical point of m_3 within at most $\mathcal{O}(\epsilon^{-3/2})$ function and derivatives' evaluations.

Under Assumption 1, Theorem 3.1 and Lemma 3.2 establishes a uniform upper and lower bound for the norm of the iterates $s^{(i)}$ for both successful and unsuccessful iterations.

Theorem 3.1. (An upper bound on step size) *Suppose that Assumption 1 holds and Algorithm 3 is employed. Then, the norm of the iterates (both successful and unsuccessful) are uniformly bounded above independently of i , such that $\|s^{(i)}\| < r_c$ for all $i \geq 0$, where r_c is a constant that depends only on the coefficients of m_3 .*

Proof. The proof of Theorem 3.1 uses a similar technique to [11, Lemma 3.2]. The proof for Theorem 3.1 is given in of Appendix B. \square

Corollary 3.1. (Upper bounding the tensor term) *Let $L_H := \Lambda_0 + 6\sigma r_c$, where*

$$\Lambda_0 := \max_{\|u_1\|=\|u_2\|=\|u_3\|=1} T[u_1][u_2][u_3].$$

Then, for every iteration, i ,

$$\|T_i\| := \max_{\|u_1\|=\|u_2\|=\|u_3\|=1} |T_i[u_1][u_2][u_3]| = \Lambda_0 + 6\sigma \|s^{(i)}\| < \Lambda_0 + 6\sigma r_c = L_H.$$

Proof. See Lemma 3.3 [14]. \square

Note that L_H is an iteration-independent constant is a constant that depends only on the coefficients in m_3 .

Lemma 3.2. (A lower bound on the step size) *Suppose that Assumption 1 holds and Algorithm 3 is used. Assume that $\|\nabla m_3(s^{(i)} + s_c^{(i)})\| > \epsilon$ and $\|g_i\| > \epsilon$, then if ⁸ $d_i \geq 0$,*

$$\|s_c^{(i)}\| > \min \left\{ (B + L_H)^{-1/2} \epsilon^{1/2}, \frac{1}{2} d_i^{-1/3} \epsilon^{1/3} \right\}. \quad (35)$$

Proof. For notational simplicity, in this proof, we use s_c to represent $s_c^{(i)}$. Since s_c is the global minimum of M_c , we have $\nabla M_c(s^{(i)}, s_c) = 0$. Thus,

$$\epsilon < \|\nabla m_3(s^{(i)} + s_c)\| = \|\nabla M(s^{(i)}, s_c)\| = \|\nabla M_c(s^{(i)}, s_c) - \nabla M(s^{(i)}, s_c)\|.$$

Using the expression of ∇M_c in (6) and $\nabla M(s^{(i)}, s) = g_i + H_i s + \frac{1}{2} T_i[s]^2 + \sigma \|s\|^2 s$, we have

$$\epsilon < \left\| \frac{1}{2} \beta_i \|s_c\| s_c - \frac{1}{2} T_i[s_c]^2 + 4d_i \|s_c\|^2 s_c \right\| \leq \frac{B}{2} \|s_c\|^2 + \frac{L_H}{2} \|s_c\|^2 + 4d_i \|s_c\|^3 \quad (36)$$

where the last inequality uses norm properties, $\beta_i > -B$ from Assumption 1 and $\|T_i\| \leq L_H$ from Corollary 3.1. If $d_i \geq 0$, either one of the following must be true

$$\frac{\epsilon}{2} < \left(\frac{B}{2} + \frac{L_H}{2} \right) \|s_c\|^2 \Rightarrow \|s_c\| > (B + L_H)^{-1/2} \epsilon^{1/2}, \quad \text{or} \quad \frac{\epsilon}{2} < 4d_i \|s_c\|^3 \Rightarrow \|s_c\| > \frac{1}{2} d_i^{-1/3} \epsilon^{1/3}$$

which gives (35). \square

⁸If $d_i = 0$, $\|s_c^{(i)}\| > (B + L_H)^{-1/2} \epsilon^{1/2}$.

Lemma 3.2 demonstrates that we can establish a lower bound for the norm of the iterates $s^{(i)}$. The lower bound on step size plays a crucial role in guaranteeing a decrease in values of m_3 . The proof incorporates standard techniques found in [4, Lemma 2.3] and in [12, Lemma 3.3], which demonstrate that the step cannot be arbitrarily small compared to the criticality conditions. It is important to note that Lemma 3.2 applies for both successful and unsuccessful iterations provided that the criticality conditions are not met, i.e., $\|\nabla m_3(s^{(i)} + s_c^{(i)})\| > \epsilon$ and $\|g_i\| \geq \epsilon$.

Theorem 3.3 provides an upper bound for m_3 at $m_3(s^{(i)} + s_c^{(i)}) = M(s^{(i)}, s_c^{(i)})$ where m_3 and M are defined in (2) and (3), respectively.

Theorem 3.3. (A local upper bound on m_3) Suppose that Assumption 1 holds and Algorithm 3 is used. Then, the following results are true.

1. **(Case 1)** If $\beta_i > L_H$, for any $d_i \geq 0$, we have $m_3(s^{(i)} + s_c^{(i)}) = M(s^{(i)}, s_c^{(i)}) \leq M_c(s^{(i)}, s_c^{(i)})$.
2. **(Case 2)** If any $\beta_i \leq L_H$ (β_i can be negative), for

$$d_i > \frac{B + L_H}{6} \|s_c^{(i)}\|^{-1} > 0, \quad (37)$$

we have $m_3(s^{(i)} + s_c^{(i)}) = M(s^{(i)}, s_c^{(i)}) \leq M_c(s^{(i)}, s_c^{(i)})$.

In both cases, the equality only happens at $s_c^{(i)} = 0$.

Proof. For notational simplicity, in this proof, we use s_c to represent $s_c^{(i)}$. By definition of M_c and M , we have

$$M_c(s^{(i)}, s_c) - M(s^{(i)}, s_c) = \frac{1}{6} \left[\beta_i \|s_c\|^3 - T_i[s_c]^3 \right] + d_i \|s_c\|^4. \quad (38)$$

If $s_c^{(i)} = 0$, clearly $M(s^{(i)}, 0) = M_c(s^{(i)}, 0)$. Assume that $\|s_c^{(i)}\| > 0$.

(Case 1) If $\beta_i \geq L_H$, for any $d_i \geq 0$, we deduce from (38) that

$$M_c(s^{(i)}, s_c) - M(s^{(i)}, s_c) \geq \frac{1}{6} \left[\underbrace{L_H - \frac{T_i[s_c]^3}{\|s_c\|^3}}_{\geq 0 \text{ by Corollary 3.1}} \right] \|s_c\|^3 + d_i \|s_c\|^4 > 0$$

(Case 2) If $\beta_i < L_H$ (β_i can be negative), we choose $d_i > \frac{1}{6}(B + L_H)\|s_c\|^{-1} > 0$. Using $\beta_i > -B$ from Assumption 1 and $T[s_c]^3 \geq -L_H\|s_c\|^3$ from Corollary 3.1, we deduce from (38) that

$$M_c(s^{(i)}, s_c) - M(s^{(i)}, s_c) > \frac{1}{6} (-B - L_H) \|s_c\|^3 + d_i \|s_c\|^4 \stackrel{(37)}{>} 0.$$

□

Remark 3.4. If d_i satisfies (37) in Theorem 3.3, then $\sigma_c^{(i)}$ satisfies the lower bound on $\sigma_c^{(i)} = \sigma + 4d_i$ in Algorithm 3, as given in (34). This is because if $d_i \geq \frac{1}{6}(B + L_H)\|s_c^{(i)}\|^{-1}$, using $B > -\beta_i$ and $L_H > 1 > \alpha > 0$, we have $d_i \geq \frac{1}{6}(-\beta_i + \alpha)\|s_c^{(i)}\|^{-1}$ and, consequently, $\sigma_c^{(i)} = \sigma + 4d_i \geq \frac{2}{3}(-\beta_i + \alpha)\|s_c^{(i)}\|^{-1}$.

Theorem 3.3 provides some intuition about how β_i approximates the third-order information. In particular, if β_i is positive and the $\beta_i\|s\|^3$ term sufficiently regularizes the third-order information, then any $d_i \geq 0$ will ensure M_c stays above m_3 . On the other hand, when β_i is negative, we need to ensure that the regularization term of M_c is large enough to guarantee $m_3(s^{(i)} + s_c^{(i)}) \leq M_c(s^{(i)}, s_c^{(i)})$. Therefore, we require d_i to satisfy (37) in Case 2.

We define the sets of successful and unsuccessful iterations for Algorithm 3 as \mathcal{S}_i and $\mathcal{U}_i = \mathcal{U}_i := [0 : i] \setminus \mathcal{S}_i$. Notice that for $i \in \mathcal{S}_i$, $\rho_j \geq \eta$ and $s^{(i+1)} = s^{(i)} + s_c^{(i)}$, while $s^{(i+1)} = s^{(i)}$ for $i \in \mathcal{U}_i$.

Lemma 3.4. (Upper bound in d_i) Suppose that Assumption 1 holds and Algorithm 3 is used. Then, for all $i \geq 0$

$$d_i \leq d_{\max} := \gamma(B + L_H)^{3/2} \epsilon^{-1/2}, \quad (39)$$

where γ is a fixed constant from Algorithm 2.

Proof. (Case 1) If $\beta_i \geq L_H$, for any $d_i \in [0, d_{\max}]$, according to Theorem 3.3, we have

$$m_3(s^{(i)}) - m_3(s^{(i)} + s_c^{(i)}) = m_3(s^{(i)}) - M(s^{(i)}, s_c^{(i)}) \geq m_3(s^{(i)}) - M_c(s^{(i)}, s_c) > 0.$$

Therefore, $\rho_i := \frac{m_3(s^{(i)}) - m_3(s^{(i)} + s_c^{(i)})}{m_3(s^{(i)}) - M_c(s^{(i)}, s_c^{(i)})} \geq 1 \geq \eta$. The iteration i is successful.

(Case 2) If $\beta_i < L_H$ (β_i can be negative) and suppose that

$$d_i \geq (B + L_H)^{3/2} \epsilon^{-1/2}.$$

We deduce that $d_i = d_i^{2/3} d_i^{1/3} \geq (B + L_H) \epsilon^{-1/3} d_i^{1/3}$. This implies the bound

$$d_i \geq (B + L_H) \max \left\{ (B + L_H)^{1/2} \epsilon^{-1/2}, d_i^{1/3} \epsilon^{-1/3} \right\} \underset{(35)}{\geq} (B + L_H) \|s_c^{(i)}\|^{-1} \quad (40)$$

where the last inequality follows from the upper bound on $\|s_c^{(i)}\|$ in Lemma 3.2. Since (40) satisfies the requirement on d_i in Theorem 3.3, we deduce that $m_3(s^{(i)} + s_c^{(i)}) \leq M_c(s^{(i)}, s_c^{(i)})$. The rest of the analysis follows similarly as in Case 1. We deduce that the iteration i is successful.

In both cases, it follows from the update of regularization parameters in Algorithm 3 that the next iteration $0 \leq d_{i+1} \leq d_i$. As a consequence, the mechanism of regularization parameters update for Algorithm 3 ensure that (39) holds. \square

Remark 3.5. It is worth noting that (34) in Algorithm 3 is below the upper bound d_{\max} ; namely, there is no contradiction between (34) and (39). To see this, assume instead that

$$\sigma_c^{(i)} = \sigma + 4d_i \geq \frac{2}{3}(-\beta_i + \alpha) \|s_c^{(i)}\|^{-1} \geq \sigma + 4d_{\max}.$$

This implies $\frac{1}{6}(-\beta_i + \alpha) \|s_c^{(i)}\|^{-1} \geq d_{\max}$. However, using $0 < \alpha < 1 \leq L_H$, the lower bound for $\|s_c^{(i)}\|$ in Lemma 3.2, d_{\max} in (39), $\gamma > 1$ and $|\beta_i| < B$, we deduce that

$$\begin{aligned} \frac{1}{6}(-\beta_i + \alpha) \|s_c^{(i)}\|^{-1} &< \frac{1}{6}(B + \alpha) \max \left\{ (B + L_H)^{1/2} \epsilon^{-1/2}, 2d_i^{1/3} \epsilon^{-1/3} \right\} \\ &< \frac{1}{3} \max \left\{ \frac{1}{2} \underbrace{(B + L_H)^{3/2} \epsilon^{-1/2}}_{=\gamma^{-1} d_{\max}}, \underbrace{(B + L_H) \epsilon^{-1/3} d_i^{1/3}}_{=\gamma^{-2/3} d_{\max}^{2/3}} \right\} \\ &< \frac{1}{3} \max \left\{ (2\gamma)^{-1}, \gamma^{-2/3} \right\} d_{\max} < d_{\max} \end{aligned}$$

which is a contraction.

The intuition behind Lemma 3.4 is that whenever the regularization parameter exceeds the bound in (39), the CQR model $M_c(s^{(i)}, s)$ overestimates m_3 at its minimizer $s = s_c^{(i)}$ (Theorem 3.3). Therefore, any decrease obtained in minimizing $M_c(s^{(i)}, s)$ is a lower bound on the decrease in m_3 , ensuring that every iteration is successful, and consequently removing the need to increase the regularization parameter any further.

Theorem 3.5. (A decrease in values of m_3 in successful iterations) Suppose that Assumption 1 holds and Algorithm 3 is used. For $\alpha \in (0, \frac{1}{2})$ and $\eta \in (0, 1]$, assume that $i + 1$ is a successful iteration which does not meet the termination condition, i.e., $\|g_{i+1}\| > \epsilon$ and $\|g_i\| > \epsilon$. Then,

$$m_3(s^{(i)}) - m_3(s^{(i+1)}) \geq \frac{\alpha\eta}{24} \|s_c^{(i)}\|^3 \geq \kappa_s \epsilon^{3/2} \quad (41)$$

where $\kappa_s = \frac{\alpha\eta}{24}(B + L_H)^{-3/2}$.

Proof. For notational simplicity, in this proof, we use s_c to represent $s_c^{(i)}$, σ_c to represent $\sigma_c^{(i)}$, and d_i to represent $d_i^{(i)}$. Since $i \in \mathcal{S}_i$, (Ratio Test) gives

$$\eta^{-1} [m_3(s^{(i)}) - m_3(s^{(i+1)})] \geq M_c(s^{(i)}, 0) - M_c(s^{(i)}, s_c) = -g_i^T s_c - \frac{1}{2} H_i[s_c]^2 - \frac{\beta_i}{6} \|s_c\|^3 - \frac{\sigma_c}{4} \|s_c\|^4$$

where $s_c^{(i)}$ is obtained by Algorithm 2 and is the global minimum of M_c . Then, $s_c^{(i)}$ satisfies (21) and (22), which implies

$$M_c(s^{(i)}, 0) - M_c(s^{(i)}, s_c) \stackrel{(21)}{=} \frac{1}{2} H_i[s_c]^2 + \frac{\beta_i}{3} \|s_c\|^3 + \frac{3\sigma_c}{4} \|s_c\|^4 \stackrel{(22)}{\geq} \frac{\beta_i}{12} \|s_c\|^3 + \frac{\sigma_c}{4} \|s_c\|^4. \quad (42)$$

- **A1):** Assuming $\beta_i \in [\alpha, B]$, since $\sigma_c > 0$, we deduce from (42) that

$$m_3(s^{(i)}) - m_3(s^{(i+1)}) \geq \frac{\beta_i\eta}{12} \|s_c\|^3 + \frac{\sigma_c\eta}{4} \|s_c\|^4 > \frac{\alpha\eta}{12} \|s_c\|^3.$$

- **A2):** Assuming $\beta_i \in [-B, \alpha]$ and $\sigma_c \geq \frac{2}{3}(-\beta_i + \alpha)\|s_c\|^{-1} > 0$, we deduce from (42) that

$$m_3(s^{(i)}) - m_3(s^{(i+1)}) \geq \frac{\beta_i\eta}{12} \|s_c\|^3 + \frac{\eta}{6}(-\beta_i + \alpha)\|s_c\|^3 \geq \left(-\frac{\beta_i}{12} + \frac{\alpha}{6}\right)\eta\|s_c\|^3 \geq \frac{\alpha\eta}{12} \|s_c\|^3.$$

where the last inequality follows from $-\beta_i \geq -\alpha$ for $\beta_i \in [-\alpha, \alpha]$ and $-\beta_i \geq \alpha$ for $\beta_i \in [-B, -\alpha]$.

- **A3):** Assuming $\beta_i \in [-B, -4\alpha]$ and $0 < \sigma_c \leq \frac{1}{6}(-\beta_i + \alpha)\|s_c\|^{-1}$: Since s_c is a global minimum, s_c is a local minimum. According to the second-order local optimality condition (7), $0 \leq \nabla^2 M_c(s^{(i)}, s_c)[s_c]^2 = H_i[s_c]^2 + \beta_i\|s_c\|^3 + 3\sigma_c\|s_c\|^4$. Substituting the local optimality condition into the middle equation in (42), we have

$$M_c(s^{(i)}, 0) - M_c(s^{(i)}, s_c) \geq -\frac{\beta_i}{6} \|s_c\|^3 - \frac{3}{4} \sigma_c \|s_c\|^4. \quad (43)$$

Using $0 < \sigma_c \leq \frac{1}{6}(-\beta_i + \alpha)\|s_c\|^{-1}$, we deduce from (43) that

$$m_3(s^{(i)}) - m_3(s^{(i+1)}) \geq -\frac{\eta\beta_i}{6} \|s_c\|^3 - \frac{\eta}{8}(-\beta_i + \alpha)\|s_c\|^3 = \left(-\frac{\beta_i}{24} - \frac{\alpha}{8}\right)\eta\|s_c\|^3 \geq \frac{\alpha\eta}{24} \|s_c\|^3$$

where the last inequality uses $\beta_i \leq -4\alpha$.

We deduce from (A1) that, in a successful step, if we have $\beta_i \in [\alpha, B]$ and $\sigma_c > 0$, then

$$m_3(s^{(i)}) - m_3(s^{(i+1)}) \geq \frac{\alpha\eta}{24} \|s_c\|^3. \quad (44)$$

Also, we can deduce from (A2) and (A3) that if $\beta_i \in [-B, -4\alpha]$ and $\sigma_c \geq \frac{2}{3}(-\beta_i + \alpha)\|s_c\|^{-1}$ or $\sigma_c \leq \frac{1}{6}(-\beta_i + \alpha)\|s_c\|^{-1}$, then (44) also holds. Lastly, using (A3), if $\beta_i \in [-4\alpha, \alpha]$ and $\sigma_c \geq \frac{2}{3}(-\beta_i + \alpha)\|s_c\|^{-1}$, then (44) also holds. These three cases correspond to the requirements of β_i and σ_c in Algorithm 3. Using the lower bound on $\|s_c\|$ in Lemma 3.2, we deduce the desired result in (41). \square

Remark 3.6. It is important to note that the $\sigma_c^{(i)}$ condition in Algorithm 3 are meant to ensure that the decrease in values of m_3 is at least $O(\epsilon^{3/2})$, specifically: $m_3(s^{(i)}) - m_3(s^{(i+1)}) \geq \frac{\alpha\eta}{24}(B+L_H)^{-3/2}\epsilon^{3/2}$. If we only have the condition $\rho_i \geq \eta$, the CQR algorithmic framework (Algorithm 2) still results in a decrease in value of m_3 at each successful iteration. This is evident from the sufficient condition for a global minimizer of M_c in Theorem 2.2, from $\beta \geq -3\sigma_c\|s_c^{(i)}\|$, we deduce that the right-hand side of (42) is positive. We can also verify the decrease in value of m_3 with the following argument. Assume $\sigma_c > 0$; the eigenvalue of H_i is bounded for all $i \geq 0$,

$$\begin{aligned}\lambda_{\max}(H_i) &= \max_{u \in \mathbb{R}^n, \|u\|=1} \left(H + T[s^{(i)}] + \sigma\|s^{(i)}\|^2 + 2\sigma(s^{(i)})^T s^{(i)} \right) [u]^2 \\ &\leq H + \Lambda_0\|s^{(i)}\| + 3\sigma\|s^{(i)}\|^2 \leq \|H\| + \Lambda_0 r_c + 3\sigma r_c^2 =: L_g\end{aligned}$$

where $\|H\| = \lambda_{\max}[H]$ and $\Lambda_0 := \max_{\|u_1\|=\|u_2\|=\|u_3\|=1} T[u_1][u_2][u_3]$. Assume that $|\beta_i| \leq B$ and set $v := -k \frac{g_i}{\|g_i\|}$ for any scalar $k > 0$. Since $s_c^{(i)}$ is the global minimizer, we have

$$\begin{aligned}M_c(s^{(i)}, 0) - M_c(s^{(i)}, s_c^{(i)}) &\geq f_i - M_c(s^{(i)}, v) = k\|g_i\| - \frac{k^2}{2} \frac{g_i^T H_i g_i}{\|g_i\|^2} - \frac{\beta_i}{6} k^3 - \frac{\sigma_c^i}{4} k^4 \\ &> k\epsilon - \frac{L_g}{2} k^2 - \frac{B}{6} k^3 - \frac{\sigma_c^i}{4} k^4 = k \left(\frac{\epsilon}{3} - \frac{L_g}{2} k \right) + k \left(\frac{\epsilon}{3} - \frac{B}{6} k^2 \right) + k \left(\frac{\epsilon}{3} - \frac{\sigma_c^i}{4} k^3 \right).\end{aligned}$$

By choosing, $0 < k < \frac{1}{2} \min \left\{ \frac{2}{3L_g}\epsilon, \left(\frac{B}{2}\epsilon\right)^{1/2}, \left(\frac{4}{3\sigma_c^i}\epsilon\right)^{1/3} \right\}$, every term in the bracket is negative, and we have

$$m_3(s^{(i)}) - m_3(s^{(i+1)}) \geq \eta \left[M_c(s^{(i)}, 0) - M_c(s^{(i)}, s_c^{(i)}) \right] \geq \frac{\epsilon k \eta}{6} > \frac{\epsilon^2 \eta}{18L_g}.$$

This analysis is unaffected by β_i being positive or negative and does not require the $\sigma_c^{(i)}$ condition in Algorithm 3.

We may now focus on how many successful iterations may be needed to compute an ϵ -approximate first-order minimizer using Algorithm 3.

Lemma 3.6. (Successful and unsuccessful adaptive-regularization iterations) Suppose that Algorithm 3 is used and that $d_i \leq d_{\max}$. Then,

$$i \leq |\mathcal{S}_i| + \frac{\log(d_{\max})}{\log \gamma}.$$

Lemma 3.6 employs a similar technique to that in [7, Lemma 2.3.1, Lemma 2.4.1], and the proof is provided in detail in Appendix C. Note that Lemma 3.6 is entirely independent of the form of the model M_c and depends on the mechanism defined by the update of regularization parameters in Algorithm 3. We do not need Assumption 1 for Lemma 3.6.

Lemma 3.7. (Bound on the number of successful iterations) Suppose that Assumption 1 holds. Let m_{low} be a lower bound on $m_3(s)$ for $s \in \mathbb{R}^n$. Then, there exists a positive constant κ_s as defined in Theorem 3.5 such that Algorithm 3 requires at most

$$|\mathcal{S}_i| := \kappa_s \frac{m_3(s^{(0)}) - m_{low}}{\epsilon^{3/2}} \quad (45)$$

successful iterations before an iterate s_ϵ is computed for which $\|g_i\| \leq \epsilon$.

Remark 3.7. Given $\sigma > 0$ as defined in (2), $m_3(s)$ is bounded below for $s \in \mathbb{R}^n$.

Proof. Suppose that $\|g_j\| > \epsilon$ and $\|g_{j+1}\| > \epsilon$ for all $j \in [1 : i]$. Then,

$$m_3(s^{(0)}) - m_{\text{low}} \geq m_3(s^{(0)}) - m_3(s^{(i+1)}) = \sum_{j \in \mathcal{S}_i} \left[m_3(s^{(j)}) - m_3(s^{(j+1)}) \right] > |\mathcal{S}_i| \kappa_s \epsilon^{3/2}$$

where κ_s given in Theorem 3.5. This implies the bound (45). \square

Given Lemma 3.7, we are now ready to state the worst-case evaluation bound for Algorithm 3.

Theorem 3.8. (Complexity bound for Algorithm 3) *Suppose that Assumption 1 holds. Then, there exists a positive constant κ_s (see Theorem 3.5), κ_c such that Algorithm 3 requires at most*

$$\kappa_s \frac{m_3(s^{(0)}) - m_{\text{low}}}{\epsilon^{3/2}} + \kappa_c + \log \epsilon^{-1/2} = O(\epsilon^{-3/2}).$$

function evaluations (i.e., f_i) and at most

$$\kappa_s \frac{m_3(s^{(0)}) - m_{\text{low}}}{\epsilon^{3/2}} + 1 = O(\epsilon^{-3/2}).$$

derivatives evaluations (i.e., g_i, H_i, T_i) to compute an iterate s_ϵ such that $\|g_i\| \leq \epsilon$ or $\|g_{i+1}\| \leq \epsilon$.

Proof. The number of successful iterations needed to find an ϵ -approximate first-order minimizer is bounded above by (45). The total number of iterations (including unsuccessful ones) can also be bounded above using Lemma 3.6, which yields that this number is at most

$$\kappa_s \frac{m_3(s^{(0)}) - m_{\text{low}}}{\epsilon^{3/2}} + \frac{\log(d_{\text{max}})}{\log \gamma} \stackrel{(39)}{=} \kappa_s \frac{m_3(s^{(0)}) - m_{\text{low}}}{\epsilon^{3/2}} + 1 + \frac{3 \log(B + L_H)}{2 \log \gamma} + \log \epsilon^{-1/2}.$$

where we use $d_{\text{max}} = \gamma(B + L_H)^{3/2} \epsilon^{-1/2}$. Since Algorithm 3 uses at most one evaluation of m_3 per iteration and at most one evaluation of its derivatives per successful iteration (plus one evaluation of m_3 and its derivatives at the final iteration), by setting $\kappa_c := 1 + \frac{3 \log(B + L_H)}{2 \log \gamma}$, we deduce the desired conclusion. \square

3.2 CQR Algorithm in Some Special Cases

Univariate m_3 : convergence of the CQR algorithm in one step. For univariate cases ($n = 1$), we define W as $W := 1$, $\sigma_c^{(0)} := \sigma$, and $\beta^{(0)} := \pm|T| \in \mathbb{R}$. We introduce two univariate CQR polynomials, denoted as $m_{c,+}$ and $m_{c,-}$, as follows:

$$m_{c,+}(s) := f_0 + gs + \frac{1}{2}Hs^2 + \frac{|T|}{6}|s|^3 + \frac{\sigma}{4}s^4, \quad m_{c,-}(s) := f_0 + gs + \frac{1}{2}Hs^2 - \frac{|T|}{6}|s|^3 + \frac{\sigma}{4}s^4.$$

As depicted in Figure 4, $m_{c,-}$ or $m_{c,+}$ overlap with m_3 in one of the half-spaces $s > 0$ or $s < 0$. Therefore, to determine the global minimum of the univariate function m_3 , our objective is to minimize the CQR polynomials $m_{c,-}$ and $m_{c,+}$. This involves finding $s_{c,+} = \operatorname{argmin}_{s \in \mathbb{R}} m_{c,+}(s)$ and $s_{c,-} = \operatorname{argmin}_{s \in \mathbb{R}} m_{c,-}(s)$ using Algorithm 1. The minimizer of m_3 is denoted as $s^* = \operatorname{argmin}_{s \in \mathbb{R}} m_3(s) = \operatorname{argmin} \{m_3(s_{c,+}), m_3(s_{c,-})\}$. We can determine the optimal value of the univariate function m_3 within a single iteration of the CQR algorithm (i.e. minimizing CQR polynomials $m_{c,-}$ and $m_{c,+}$ once each). An illustrative example of this minimization process is presented in Figure 4, where the global minimizer for $m_3(s)$ aligns with that of $m_{c,+}(s)$.

In the multivariate case ($n \geq 2$), the tensor directions are not restricted to $s \geq 0$ or $s \leq 0$ as they are in the univariate case. Therefore, it is generally not possible to find a choice of $m_{c,\pm}(s)$

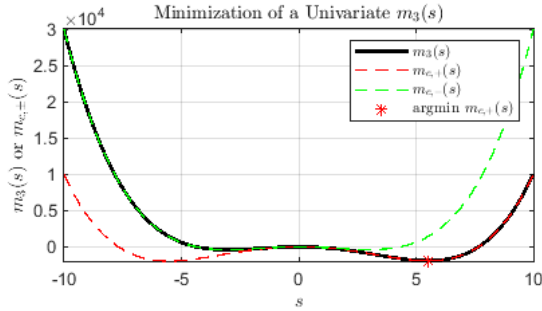


Figure 4: Minimization of univariate $m_3(s) = 3s - 50s^2 - 10s^3 + 3s^4$.

that is equal to $m_3(s)$. However, similar to the univariate case, we can formulate the half plane as $\mathcal{H}_+ = \{s_c^{(i)} \in \mathbb{R}^n, T[s_c^{(i)}]^3 \geq 0\}$ and $\mathcal{H}_- = \{s_c^{(i)} \in \mathbb{R}^n, T[s_c^{(i)}]^3 < 0\}$. Our aim is to choose $\beta_i \approx \frac{T[s_c^{(i)}]^3}{\|s_c^{(i)}\|}$. More details can be found in Section 4.

Diagonal Hessian and Tensor: Suppose that $H = \nabla^2 f(x_k)$ and $T = \nabla^3 f(x_k)$ are diagonal matrices and tensors with diagonal entries $D_\iota \in \mathbb{R}$ and $\tilde{T}_\iota \in \mathbb{R}$ for $\iota = 1, \dots, n$, respectively. By incorporating a slightly different fourth-order regularization norm, namely $\sigma \|s\|_4^4 = \sigma \sum_{i=1}^n s_i^4$ with $\sigma > 0$, we can obtain a separable cubic-quartic polynomial denoted as

$$\tilde{m}_3(s) := f_0 + g^T s + \frac{1}{2} H[s]^2 + \frac{1}{6} T[s]^3 + \sigma \|s\|_4^4 = f_0 + \underbrace{\sum_{\iota=1}^n \left[g_\iota s_\iota + \frac{1}{2} D_\iota s_\iota^2 + \frac{1}{6} \tilde{T}_\iota s_\iota^3 + \frac{\sigma}{4} s_\iota^4 \right]}_{\text{univariate CQR Polynomial}}.$$

Here, $s_\iota \in \mathbb{R}$ and $g_\iota \in \mathbb{R}$ denote the ι th entry of the vectors $s \in \mathbb{R}^n$ and $g \in \mathbb{R}^n$, respectively. Consequently, we expressed $\tilde{m}_3(s)$ as the sum of n univariate CQR polynomials, and minimizing $\tilde{m}_3(s)$ can be reduced to the minimization of n separate univariate CQR polynomials. Each of these polynomials can be efficiently solved using a single step of the univariate CQR algorithm.

Small Tensor Term: If the tensor term is small, $\|T_i\| \leq \epsilon^{1/3}$, and we also choose $|\beta_i| \leq \epsilon^{1/3}$, then (36) becomes $\epsilon < \frac{\epsilon^{1/3}}{2} \|s_c\|^2 + \frac{\epsilon^{1/3}}{2} \|s_c\|^2 + 4d_i \|s_c\|^3$. This inequality implies $\|s_c^{(i)}\| > O(\epsilon^{1/3})$. Following the analysis in Theorem 3.5, this results in a complexity bound of order $O(\epsilon)$.

4 Numerical Implementation and Preliminary Results

In this section, we present the implementation of CQR method and provide preliminary numerical results of the algorithm. The CQR Variant for numerical implementation is described in Algorithm 4.

When comparing the CQR Variant for numerical implementation (Algorithm 4) to the CQR algorithmic framework (Algorithm 2), it is worth noting that Algorithm 2 does not specify a particular choice for β_i , whereas Algorithm 4 offers three options for updating β_i that we can choose from. The three choices are summarised as follows.

The first choice of β_i in Algorithm 4 stems from our theoretical analysis in Theorem 3.3 and Corollary 3.1. By setting $\beta_i = L_H(s^{(i)}) = \Lambda_0 + 6\sigma \|s^{(i)}\|$ where Λ_0 is calculated as in [6, Thm 2.6], we ensure that $M(s^{(i)}, s_c^{(i)}) \leq M_c(s^{(i)}, s_c^{(i)})$ for all i . This guarantees that $\rho_i > 1$ in every iteration of Algorithm 4, namely every step is a successful step. A numerical example of this choice of β_i is given in Figure 5 where we plot the value of β_i , the size of d_i , and the performance ratio for both successful and unsuccessful iterations. Our experimental findings affirm our theoretical results that each iteration indeed satisfies $\rho_i \geq 1$ (right plot of Figure 5). Consequently, there are no unsuccessful

Algorithm 4: A CQR Variant for Numerical Implementation

Initialize and proceed through Steps 1 to 4 of the CQR algorithmic framework (Algorithm 2).

Specifically, in each iteration (i), compute $s_c^{(i)} := \operatorname{argmin}_{s \in \mathbb{R}^n} M_c(s^{(i)}, s)$, where β_i is initialised and updated using one of the following updating rules:

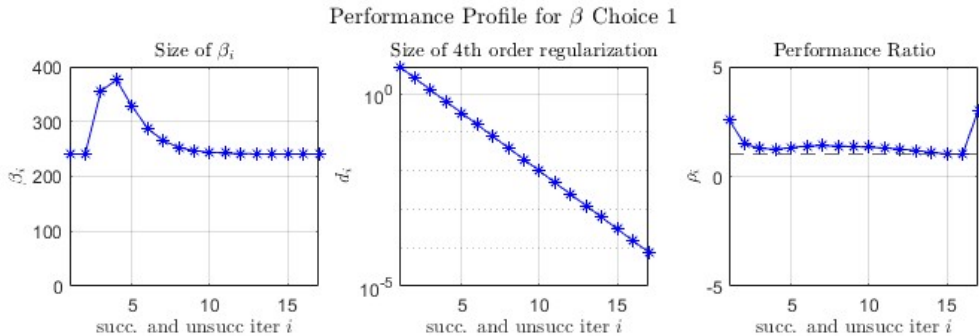
1. $\beta_{i+1} := L_H(s^{(i)}) = \Lambda_0 + 6\sigma \|s^{(i)}\|$ for $i \geq 0$; $\beta_0 := \Lambda_0 = \sqrt{\sum_l \max_{1 \leq j, k \leq n} T[l, j, k]^2}$.
2. $\beta_{i+1} := \frac{T_i[s_c^{(i)}]^3}{\|s_c^{(i)}\|^3}$ for $i \geq 0$; $\beta_0 := -\max_{1 \leq j \leq n} |T[j, j, j]|$.
3. $\beta_{i+1} := \frac{1}{n} \sum_{j=i}^n T_i[j, j, j]$ for $i \geq 0$; $\beta_0 := -\max_{1 \leq j \leq n} |T[j, j, j]|$.

In choices 2 or 3 above: initialise an upper bound $B > 0$ at the start of the algorithm; at iteration (i), if $|\beta_{i+1}| > B$, then set^b $\beta_{i+1} := \operatorname{sign}(\beta_{i+1})B$.

^bSee Remark 4.1.

iterations. Furthermore, as each iteration achieves $\rho_i \geq 1$, which is considered as ‘a very successful step’, we observe a reduction in d_i by a factor of γ_2 per iteration (the second plot of Figure 5). In the last few iterations, d_i has magnitude 10^{-3} , nearly reaching zero, while the iterations remain successful.

Figure 5: Performance profile of Algorithm 4 using the first choice of β_i . The detailed setup of the test problem is in Section 4.1.1 and parameters in (46) are set at $\mathbf{a} = 80$, $\mathbf{b} = 80$, $\mathbf{c} = 80$, $\sigma = 5$, and $n = 100$.



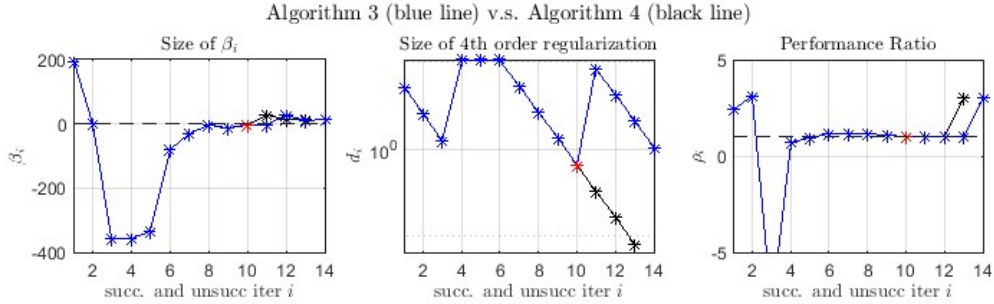
The second and third choices of β_i in Algorithm 4 are the practical ones for efficient algorithm implementation. In subsequent sections, we conduct numerical tests using one of these two choices. The second choice of β_i in Algorithm 4 is derived from the observation in (38). For each iteration, Theorem 3.3 holds if the condition $\beta_{i+1} \geq T_i[s_c^{(i+1)}]^3 \|s_c^{(i+1)}\|^{-3}$ is satisfied. However, prior to minimizing $M_c(s^{(i)}, s)$, $s_c^{(i)}$ remains unknown. Therefore, in the algorithmic implementation, we update the $\beta_{i+1} := T_i[s_c^{(i)}]^3 \|s_c^{(i)}\|^{-3}$ which is the tensor applied to the search direction from the last successful iteration. We use this update as an estimate of $T_i[s_c^{(i+1)}]^3 \|s_c^{(i+1)}\|^{-3}$. For the third choice of β_i in Algorithm 4, we opt for β_i to be the scaled trace of T_i : $\beta_{i+1} := \frac{1}{n} \sum_{j=i}^n T_i[j, j, j]$. Preliminary examples for these two choices of β_i are provided in Appendix D.

When contrasting the CQR Variant for numerical implementation (Algorithm 4) with the CQR variant featuring optimal complexity (Algorithm 3), a notable distinction arises. Unlike the Algorithm 3, Algorithm 4 does not have the additional requirement on $\sigma_c^{(i)}$, thereby allowing for a more adaptive choice of $\sigma_c^{(i)}$. In other words, Algorithm 3 adopts a more conservative approach when accepting steps compared to Algorithm 4. Yet, according to the analysis presented in Remark 3.6, Algorithm 4 ensures a reduction in the value of m_3 during each successful iteration and converges to a point satisfying $\|g_i\| < \epsilon$. A numerical example comparing Algorithm 3 and Algorithm 4 is given in Figure

6.

Remark 4.1. In Assumption 1, we assume that β_i is bounded for all iterations. In Algorithm 4, the parameter B prevents $|\beta_i|$ from becoming excessively large, thereby averting potential numerical instability.

Figure 6: Performance comparison between Algorithm 3 and 4 with the second choice of β_i and $\alpha = 0.1$: Algorithm 3 uses 14 total iterations while Algorithm 4 uses 13 total iterations. The differences in iterations between the two algorithms are with a red asterisk $*$. The same test example is used as in Figure 5.



Choices 1–3 for updating β_i in Algorithm 4 are just a few options within the general CQR framework. Other methods of selecting β_i are also possible. For example, one could use β_i as the smallest or largest eigenvalue of the tensor, the smallest or largest entries of T , or update β_i in an unsuccessful step. Further investigation into these β_i choices will be pursued in future research.

4.1 Numerical Results: Comparison Across Methods

In this section, we carry out numerical experiments for CQR algorithm (Algorithm 4) with practical β choices (Choices 2 or 3). To assess the performance of CQR solvers, we devise multiple sets of AR3 subproblems across different dimensions, n , ranging from 5 to 100. These test sets comprise AR3 subproblems with varying gradients, Hessians, tensors, and regularization terms. Specifically, we consider singular, ill-conditioned, indefinite, and diagonal Hessians, as well as large and small tensor terms, diagonal tensor terms, badly scaled tensor terms, and dense tensor terms. We also provide examples arising from the minimization of multi-dimensional objective functions that illustrate further aspects of CQR method’s performance.

4.1.1 Numerical Set-up

The test sets are constructed as follows: we generate quartic regularized polynomials to assess the algorithm’s performance. Specifically, we define $m_3(s) = f_0 + g^T[s] + \frac{1}{2}H[s]^2 + \frac{1}{6}T[s]^3 + \frac{1}{4}\sigma\|s\|_2^4$, where $f_0 = 0$, and the coefficients g , H , and T are generated as follows:

$$g = \mathbf{a} * \text{randn}(n, 1), \quad H = \mathbf{b} * \text{symm}(\text{randn}(n, n)), \quad T = \mathbf{c} * \text{symm}(\text{randn}(n, n, n)) \quad (46)$$

Here, n represents the dimension of the problem ($s \in \mathbb{R}^n$), and $\text{symm}(\text{randn}())$ denotes a symmetric matrix or tensor with entries following a standard normal distribution with mean zero and variance one. The parameters \mathbf{a} , \mathbf{b} , \mathbf{c} , and σ are selected differently to test the algorithm’s performance under various scenarios. We set the stopping criterion to be $\|g_i\| < \epsilon$, where $\epsilon = 10^{-5}$ unless otherwise specified. The parameters in Algorithm 2 are set as $\eta_1 = 0.9$, $\eta = 0.1$, $\gamma_2 = 0.5$, $\gamma = 2.0$ and

$B = \max_{1 \leq \ell, j, k \leq n} |T[\ell, j, k]|$. The iteration counts include both successful and unsuccessful iterations. The counts of function and derivative evaluations match the number of successful iterations. It is worth noting that the CQR algorithm (Algorithm 4) is tensor-free and does not require information about the tensor entries or its structure. Instead, the algorithm only requires tensor-vector and tensor-matrix products.

4.1.2 Comparison Across Methods

In this section, we give a comparison of several minimization algorithms for the AR3 subproblem. These algorithms encompass the ARC method, Nesterov’s method (specifically for convex m_3), QQR-v1 method, and QQR-v2 method. The ARC method, as proposed in Cartis et al. [8], forms the basis of this comparison. Nesterov’s method, introduced in [32], is tailored for convex subproblems only. The QQR method, a recent development introduced in [14], can be considered as a nonconvex generalization of Nesterov’s method; it approximates the third-order tensor term through a linear combination of quadratic and quartic terms. In our numerical testing, we assess both variants of QQR (QQR-v1 and QQR-v2). QQR-v1 follows a framework similar to Nesterov’s method, employing a single adaptive parameter to govern the quadratic and quartic terms. In contrast, QQR-v2 employs two adaptive parameters to manage the convexity scenario and regularization magnitude, respectively.

The numerical results (Tables 2–6 in Appendix E) consistently demonstrate that our proposed methods, the CQR method (with β choices 2 or 3 in Algorithm 4), perform competitively with the ARC method and the Nesterov’s method. In particular, CQR methods typically require fewer evaluations of functions/derivatives or iterations than the ARC method, Nesterov’s method, and QQR-v1. Moreover, CQR methods exhibit robustness when handling ill-conditioned Hessian terms and perform effectively for minimizing m_3 with singular or diagonal Hessians (Table 3). In the case of convex and locally strictly convex m_3 functions (Table 2), the CQR algorithm (Algorithm 4) terminates within only a few iterations and function evaluations. Notably, in these scenarios, the CQR method requires fewer iterations and evaluations to converge than Nesterov’s method (which is specifically for convex m_3). The primary reason is that our implementation of the CQR method employs β_i to estimate the tensor direction, whereas Nesterov’s method (and QQR-v1) solely utilizes a single-parameter linear combination of the local upper and lower bounds. Furthermore, the CQR method effectively locates a point satisfying $\|g_i\| < \epsilon$ for quartic polynomials characterised by diagonal tensor terms, and large, negative, directional tensors (Tables 5–6). Lastly, our proposed algorithm successfully identifies a point satisfying $\|g_i\| < \epsilon$ across a wide range of positive σ values (Table 4), allowing for dynamic σ adjustments while employing CQR method to solve the AR3 problem.

4.1.3 CQR Performance in Challenging Scenarios

As observed in Table 2 to Table 6, for well-scaled subproblems, CQR methods tend to perform comparably with the QQR-v2 method in terms of iterations and function evaluations. However, we have noticed that in certain practical problems, such as Problem 4 of Moré, Garbow, and Hillstom’s test set [27], known as the Brown badly scaled problem, our investigation revealed a significant performance advantage of CQR when compared to ARC and QQR. We solved this problem using the AR3 method as described in [12] by minimizing (AR3 Model) with various subproblem solvers and compared their performances. The performance comparison is provided in Table 1. We observe that the AR3 method

with the CQR subproblem solver requires only approximately 2 iterations (or evaluations) per subproblem to converge, while the AR3 method in (AR3 Model) with the ARC or QQR subproblem solver requires at least three times the iterations (or evaluations). After examining the subproblem linked to this challenging scenario, we noticed that the gradient, Hessian, and tensor exhibited significantly larger magnitudes in a specific entry (or in a few entries), while all other entries remained relatively small, typically around a magnitude of 1. Furthermore, the search directions were usually predominantly influenced by these tensor directions.

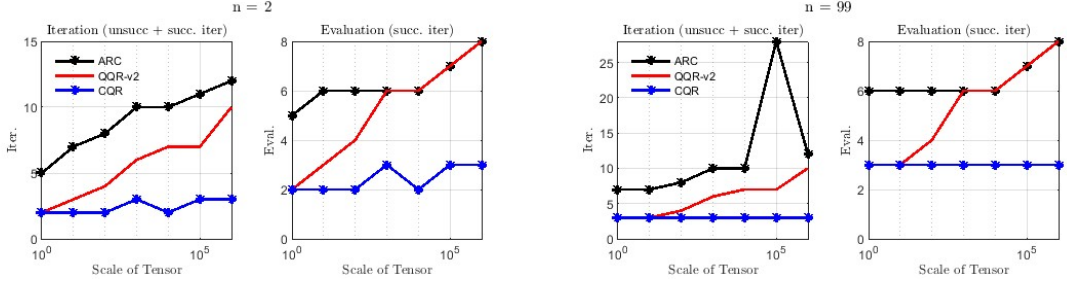
Table 1: The objective function to minimize is Problem 4 of Moré, Garbow, and Hillstom’s test set, known as the Brown badly scaled problem. The first-order optimality tolerances for minimizing the objective function and the subproblem are 10^{-4} and 10^{-5} respectively, and the initialization is $x_0 = \mathbf{0}$ with $\sigma = 1$. The AR3 model is outlined in (AR3 Model), more details can be found in [12].

Method	No. of iterations per subproblem	
	Total Iter.	Successful Iter.
AR3 with ARC	16.4	6.3
AR3 with QQR-v2	10.3	10.2
AR3 with CQR-Choice 2	1.9	1.9
AR3 with CQR-Choice 3	1.9	1.9

Given these challenging conditions, we conducted a series of tests to assess the performance of the CQR solver in handling such badly scaled problems. We first design a test scenario where all other entries in g , H , and T were set to 0, with only the first diagonal entry varying in magnitude from 0.1 to 10^5 . In these examples, as illustrated in the right two plots of Figure 10 in Appendix F, CQR converges in just 1 or 2 iterations, whereas ARC and QQR-v2 required 6 to 15 iterations. It is noteworthy that in this problem, the CQR method is also relatively insensitive to the problem size. Specifically, the CQR method converges within a few iterations throughout all dimensions. We attribute this behaviour to the problem’s strong dependence on the direction characterised by the largest tensor entry. The successful identification of a point that satisfies $\|g_i\| < \epsilon$ was closely linked to how effectively the algorithms progressed along the dominant tensor direction. The CQR method excelled in efficiency in these cases.

We could also add random perturbations to the zero entries of the g , H , and T . We choose the gradient, Hessian, and tensors with entries of relatively small magnitudes, randomly following a normal distribution with mean zero and variance 0.1, while the first entry of g , H , and T was systematically varied from small to large magnitudes in the same direction. We tested these scenarios on subproblems ranging in size from $n = 2$ to $n = 100$. As illustrated in Figure 7, when the tensor term is well-scaled, QQR-v2 and the CQR method perform similarly. However, as the magnitude of the first entry increases, signifying a shift in the descent direction toward dominance by the tensor direction T , the CQR method starts to outperform ARC and QQR-v2 in terms of both iteration and evaluation counts. In particular, for a tensor scaling of 10^6 , the CQR algorithm (Algorithm 4) terminates in just 4 iterations, while ARC and QQR-v2 require 10 to 25 iterations. This improvement could be primarily attributed to the β parameter, which effectively captures the dominant tensor direction that exerts a substantial influence on the subproblem.

Figure 7: Performance profile of a badly scaled problem: the first entry of g , H , and T scales from -0.1 to -10^5 , while the rest of the entries follow a normal distribution $\mathcal{N}(0, 0.1)$, and $\sigma = 50$. The left two plots have dimension $n = 2$, and the right two plots have dimension $n = 100$. The tensor scale is defined as the maximum absolute value of the tensor entries divided by the mean absolute value of tensor entries. β_i is chosen as per choice 2 in Algorithm 4), with similar performance observed for β_i as per choice 3 (Figure 11 in Appendix F).



In our exploration of additional examples, we also considered scenarios where the first diagonal entry was large, and we introduced variations in some off-diagonal entries of the tensor T (Figure 12 Appendix F). As expected, similar trends are observed, as the descent direction of m_3 remains predominantly influenced by the diagonal tensor direction T . When we expanded our experiments to include more entries with large magnitudes, the performance of CQR began to match that of QQR-v2 and ARC. This behaviour was attributed to the introduction of multiple large diagonal entries in T , resulting in a higher rank tensor. The CQR method, with its single β parameter, faces limitations in capturing all the tensor directions introduced.

5 Conclusions and Future Work

In conclusion, this paper introduces the CQR method, designed for the efficient minimization of nonconvex quartically-regularized cubic polynomials, such as the AR3 subproblem. The CQR method iteratively minimizes a local quadratic model incorporating cubic and quartic terms, known as the CQR polynomial. The cubic term has a coefficient β_i that provides crucial information about the local tensor $T_i[s]^3$, while the quartic term has a coefficient σ_c that controls the regularization and algorithmic progress. We have derived necessary and sufficient global optimality conditions for the global minimizer of the CQR polynomial. These conditions allow us to transform the problem of finding the global minimizer of the CQR polynomial into a more manageable nonlinear eigenvalue problem. Future research may explore the convergence of the root-finding algorithm for this system and scalable techniques for solving it.

Our theoretical analysis affirmed the convergence of the CQR method, showing that it is guaranteed to find a first-order critical point for the AR3 subproblem within at most $\mathcal{O}(\epsilon^{-3/2})$ function and derivative evaluations; here, ϵ represents the prescribed first-order optimality tolerance. The complexity bound for the CQR method is as least as good as that of ARC, and in specific cases, it exhibits improved convergence behaviour. Preliminary numerical results also suggest competitive performance by our tensor-free CQR method when compared to state-of-the-art approaches such as the ARC method, often requiring fewer iterations or evaluations. Notably, our findings particularly highlight the CQR method's performance on badly scaled problems, where it outperformed other approaches like ARC and QQR in terms of both iteration and evaluation counts.

The proposed CQR methods offer a way to approximate the third-order tensor term by a single cubic term. In the future, we plan to incorporate additional tensor information into cubic terms in CQR-like models, to capture third-order directions more accurately. By proposing efficient AR3 minimization algorithms, this paper brings high-order tensor methods closer to practical applications.

A Derivative for $\Psi(\lambda)$

Let $H_W(\lambda) = H_i + \lambda W$ and $W^{-1}H_W(\lambda)$ has the Cholesky factorization

$$W^{-1}H_W(\lambda) = L(\lambda)L^T(\lambda). \quad (47)$$

Differentiate $(H_i + \lambda W)s(\lambda) = -g_i$ against λ gives $(H_i + \lambda W)\nabla_\lambda s(\lambda) + Ws(\lambda) = 0$. Therefore,

$$\nabla_\lambda s(\lambda) = -H_W^{-1}(\lambda)Ws(\lambda). \quad (48)$$

On the other hand, $\Psi(\lambda) = \|s(\lambda)\|_W^2$ has derivative $\Psi'(\lambda) = 2\langle Ws(\lambda), \nabla_\lambda s(\lambda) \rangle$. Substituting (47) and (48) gives,

$$\begin{aligned} \Psi'(\lambda) &= -2\langle Ws(\lambda), L(\lambda)^{-T}L^{-1}(\lambda)s(\lambda) \rangle \\ &= -2\langle L(\lambda)^{-1}Ws(\lambda), L(\lambda)^{-1}s(\lambda) \rangle = -2\|L(\lambda)^{-1}s\|_W = -2\|\omega(\lambda)\|_W^2. \end{aligned}$$

where $L(\lambda)\omega(\lambda) = s(\lambda)$.

B Uniform Upper Bound for Iterates

In this section, we prove that the iterates of Algorithm 2, including both successful and unsuccessful iterations, are uniformly bounded above by a constant r_c independent of the iteration count. The constant r_c is determined by the coefficients in m_3 , specifically f_0 , g , H , and T . We first require a technical lemma.

Lemma B.1. *Let M_c be defined as in (CQR Model) in Algorithm 2 with $d_i \geq 0$. Denote $\hat{s} := s^{(i)} + s$. If $\|\hat{s}\| = \|s^{(i)} + s\| \geq \|s^{(i)}\|$, then*

$$M_c(s^{(i)}, s) \geq \underbrace{f_0 + g^T[s^{(i)} + s] + \frac{1}{2}H[s^{(i)} + s]^2 + \frac{1}{6}T[s^{(i)} + s]^3}_{=T_3(\hat{s})} - \frac{1}{6}T[s]^3 + \frac{\beta_i}{6}\|s\|^3 + \frac{\sigma}{20}\|s^{(i)} + s\|^4.$$

Proof. Using the condition $\|s^{(i)} + s\| \geq \|s^{(i)}\|$, we obtain that

$$\|s^{(i)}\|^2 + \|s\|^2 + 2s^T s^{(i)} \geq \|s^{(i)}\|^2 \quad \Rightarrow \quad s^T s^{(i)} + \frac{1}{2}\|s\|^2 \geq 0. \quad (49)$$

Also, by Taylor expansion at $s = s^{(0)} = 0$,

$$\begin{aligned} f_i &= m_3(s^{(i)}) = f_0 + g^T s^{(i)} + \frac{1}{2}H[s^{(i)}]^2 + \frac{1}{6}T[s^{(i)}]^3 + \frac{\sigma}{4}\|s^{(i)}\|^4, \\ g_i^T s &= \nabla m_3(s^{(i)}) = g^T s + H[s^{(i)}][s] + \frac{1}{2}T[s^{(i)}]^2[s] + \sigma\|s^{(i)}\|^2 s^T s^{(i)}, \\ H_i[s]^2 &= \nabla^2 m_3(s^{(i)}) = H[s]^2 + T[s^{(i)}][s]^2 + \sigma\|s^{(i)}\|^2\|s\|^2 + 2\sigma[s^T s^{(i)}]^2. \end{aligned}$$

Substituting the above expressions into $M_c(s^{(i)}, s) = f_i + g_i^T s + \frac{1}{2}H[s_i]^2 + \frac{\beta}{6}\|s\|^3 + \frac{\sigma_c}{4}\|s\|^4$ and rearranging, we have

$$\begin{aligned} M_c(s^{(i)}, s) &= f_0 + g^T(s^{(i)} + s) + \frac{1}{2}\left(H[s^{(i)}]^2 + 2H[s^{(i)}][s] + H[s]^2\right) + \\ &\quad + \frac{1}{6}\left(T[s^{(i)}]^3 + 3T[s^{(i)}]^2[s] + 3T[s^{(i)}][s]^2 + \beta_i\|s\|^3\right) + \\ &\quad + \frac{\sigma}{4}\left(\|s^{(i)}\|^4 + 4\|s^{(i)}\|^2 s^T s^{(i)} + 2\|s^{(i)}\|^2\|s\|^2 + 4[s^T s^{(i)}]^2 + \|s\|^4\right) + d_i\|s\|^4. \end{aligned}$$

Using $T[s^{(i)} + s]^3 - T[s]^3 = T[s^{(i)}]^3 + 3T[s]^2[s^{(i)}] + 3T[s^{(i)}]^2[s]$ and $\|s^{(i)} + s\|^4 = \|s^{(i)}\|^4 + 4\|s\|^2 s^T s^{(i)} + 2\|s\|^2\|s^{(i)}\|^2 + 4[s^T s^{(i)}]^2 + 4\|s^{(i)}\|^2 s^T s^{(i)} + \|s\|^4$, we deduce that

$$\begin{aligned} M_c(s^{(i)}, s) &= f_0 + g^T[s^{(i)} + s] + \frac{1}{2}H[s^{(i)} + s]^2 + \frac{1}{6}\left(T[s^{(i)} + s]^3 - T[s]^3 + \beta_i\|s\|^3\right) + \frac{\sigma}{20}\|s^{(i)} + s\|^4 \\ &\quad + \frac{\sigma}{5}\left(\underbrace{\|s^{(i)}\|^4 + 4\|s^{(i)}\|^2 s^T s^{(i)} + 2\|s\|^2\|s^{(i)}\|^2 + 4[s^T s^{(i)}]^2 + \|s\|^4 - \|s\|^2 s^T s^{(i)}}_{\geq 0 \text{ by (49)}}\right) + \underbrace{d_i\|s\|^4}_{\geq 0}. \end{aligned}$$

I_4

Note that

$$I_4 \geq \|s^{(i)}\|^4 + 4[s^T s^{(i)}]^2 + \|s\|^4 - \|s\|^2 s^T s^{(i)} \geq \|s\|^4 - \|s\|^3\|s^{(i)}\| + \|s^{(i)}\|^4.$$

If $\|s\| \leq \|s^{(i)}\|$, the sum of the last two terms is positive. If $\|s\| \geq \|s^{(i)}\|$, the sum of the first two terms is positive. In both cases, $I_4 \geq 0$, thus, we obtained the desired result. \square

Now, we are ready to prove that the iterates generated by Algorithm 2 are uniformly bounded.

Theorem B.2. *Let M_c be defined as in (CQR Model) with $d_i \geq 0$ and $|\beta_i| \leq B$. Suppose that the CQR algorithmic framework (Algorithm 2) or its variants are used with $s^{(0)} = 0$ and $s_c^{(i)} = \operatorname{argmin}_{s \in \mathbb{R}^n} M_c(s^{(i)}, s)$. Then, for all $i \geq 0$,*

$$\|s^{(i)} + s_c^{(i)}\| < r_c := \max \left\{ \left(\frac{60\|g\|}{\sigma} \right)^{1/3}, \left(\frac{30\|H\|}{\sigma} \right)^{1/2}, \left(\frac{80B}{\sigma} + \frac{90\Lambda_0}{\sigma} \right) \right\} \quad (50)$$

where $\|g\| = \sqrt{g^T g}$, $\|H\| = \max_i |\lambda_i(H)|$ is the maximum absolute value of eigenvalues of H and $\Lambda_0 := \|T\| = \max_{\|u_1\|=\|u_2\|=\|u_3\|=1} T[u_1][u_2][u_3]$.

Remark B.1. *Note that r_c is an iteration-independent bound and only depends on g , H , T , and B , which are fixed for m_3 . The only requirement for Theorem B.2 is that $|\beta_i| \leq B$, where B is a positive constant (i.e., the coefficients of the cubic-order term of M_c are uniformly bounded), and $m_3(s^{(i)}) \leq m_3(s^{(0)})$. The proof of Theorem B.2 does not require the performance ratio test and is thus valid for both successful and unsuccessful iterations.*

Proof. We prove the desired result by induction. For $i = 0$, $s^{(0)} = 0$, $M_c(s^{(0)}, 0) = f_0$, $s_c^{(0)} = \operatorname{argmin}_{s \in \mathbb{R}^n} M_c(s^{(0)}, s)$. Clearly, $0 \geq M_c(s^{(0)}, s_c^{(0)}) - f_0$. Therefore,

$$0 \geq g^T s_c^{(0)} + \frac{1}{2}H[s_c^{(0)}]^2 + \frac{\beta_0}{6}\|s_c^{(0)}\|^3 + \frac{\sigma}{4}\|s_c^{(0)}\|^4 \geq -\|g\|\|s_c^{(0)}\| - \frac{\|H\|}{2}\|s_c^{(0)}\|^2 - \frac{B}{6}\|s_c^{(0)}\|^3 + \frac{\sigma}{4}\|s_c^{(0)}\|^4$$

where the second inequality uses the Cauchy-Schwarz inequality, norm properties, and $\beta_0 > -B$. We further deduce that

$$0 \geq \left(-\|g\| + \frac{\sigma}{12}\|s_c^{(0)}\|^3 \right) \|s_c^{(0)}\| + \left(-\frac{\|H\|}{2} + \frac{\sigma}{12}\|s_c^{(0)}\|^2 \right) \|s_c^{(0)}\|^2 + \left(-\frac{B}{6} + \frac{\sigma}{12}\|s_c^{(0)}\| \right) \|s_c^{(0)}\|^3.$$

The inequality above cannot hold unless at least one of the terms on the right-hand side is negative, which is equivalent to

$$\|s^{(0)} + s_c^{(0)}\| \leq \max \left\{ \left(\frac{12\|g\|}{\sigma} \right)^{1/3}, \left(\frac{6\|H\|}{\sigma} \right)^{1/2}, \frac{2B}{\sigma} \right\} < r_c.$$

Thus, (50) is true for $i = 0$.

For the inductive hypothesis⁹, assume (50) is true at the $(i-1)$ th iteration $\|s^{(i-1)} + s_c^{(i-1)}\| \leq r_c$.

At the i th iteration, either we are in the good case, $\|s^{(i)} + s_c^{(i)}\| \leq \|s^{(i)}\|$ which leads to $\|s^{(i)} + s_c^{(i)}\| \leq \|s^{(i)}\| \leq r_c$ directly. Or, we are in the hard case, $\|s^{(i)} + s_c^{(i)}\| \geq \|s^{(i)}\|$. In this case, since $s_c^{(i)} = \operatorname{argmin}_{s \in \mathbb{R}^n} M_c(s^{(i)}, s)$, we have $0 \geq M_c(s^{(i)}, s_c^{(i)}) - M_c(s^{(i)}, 0) = M_c(s^{(i)}, s_c^{(i)}) - f_i \geq \dots \geq M_c(s^{(i)}, s_c^{(i)}) - f_0$. Denoting $\hat{s} := s^{(i)} + s_c^{(i)}$, using Lemma B.1, we have

$$\begin{aligned} 0 &\geq M_c(s^{(i)}, s_c^{(i)}) - f_0 \geq g^T \hat{s} + \frac{1}{2} H[\hat{s}]^2 + \frac{1}{6} T[\hat{s}]^3 - \frac{1}{6} T[s_c^{(i)}]^3 + \frac{\beta_i}{6} \|s_c^{(i)}\|^3 + \frac{\sigma}{20} \|\hat{s}\| \\ &> -\|g\| \|\hat{s}\| - \frac{\|H\|}{2} \|\hat{s}\|^2 - \frac{\Lambda_0}{6} \|\hat{s}\|^3 - \frac{\Lambda_0}{6} \|s_c^{(i)}\|^3 - \frac{B}{6} \|s_c^{(i)}\|^3 + \frac{\sigma}{20} \|\hat{s}\|^4. \end{aligned}$$

The last inequality uses the Cauchy-Schwarz inequality, norm properties, and $\beta_i > -B$. Since $\|\hat{s}\| \geq \|s^{(i)}\|$, this gives $\|s_c^{(i)}\| = \|\hat{s} - s^{(i)}\| \leq \|\hat{s}\| + \|s^{(i)}\| \leq 2\|\hat{s}\|$. Consequently,

$$\begin{aligned} 0 &> -\|g\| \|\hat{s}\| - \frac{\|H\|}{2} \|\hat{s}\|^2 - \frac{3\Lambda_0}{2} \|\hat{s}\|^3 - \frac{4B}{3} \|\hat{s}\|^3 + \frac{\sigma}{20} \|\hat{s}\|^4 \\ &= \left(-\|g\| + \frac{\sigma}{60} \|\hat{s}\|^3 \right) \|\hat{s}\| + \left(-\frac{\|H\|}{2} + \frac{\sigma}{60} \|\hat{s}\|^2 \right) \|\hat{s}\|^2 + \left(-\frac{4B}{3} - \frac{3\Lambda_0}{2} + \frac{\sigma}{60} \|\hat{s}\| \right) \|\hat{s}\|^3. \end{aligned}$$

The inequality above cannot hold unless at least one of the terms on the right-hand side is negative, which is equivalent to $\|s^{(i)} + s_c^{(i)}\| = \|\hat{s}\| \leq \max \left\{ \left(\frac{60\|g\|}{\sigma} \right)^{1/3}, \left(\frac{30\|H\|}{\sigma} \right)^{1/2}, \left(\frac{80B}{\sigma} + \frac{90\Lambda_0}{\sigma} \right) \right\} = r_c$. \square

C Proof of Lemma 3.6

Proof. The update of regularization parameters in Algorithm 3 gives that, for each i ,

$$0 \leq d_{j+1} \leq d_j, \quad j \in \mathcal{S}_i, \quad \gamma \max\{1, d_j\} = d_{j+1}, \quad j \in \mathcal{U}_i,$$

where $j \in [0 : i]$. Using $d_0 = 0$, we inductively deduce that $\gamma^{|U_i|} = \max\{1, d_0\} \gamma^{|U_i|} \leq d_i$. Therefore, using our assumption that $d_i \leq d_{\max}$, we deduce that

$$|U_i| \log \gamma \leq \log(d_{\max}).$$

The desired result follows from the inequality $i = |U_i| + |S_i|$. \square

⁹This is the same as $\|s^{(i-1)}\| = \|s^{(i-1)} + s_c^{(i-1)}\| \leq r_c$ if iteration is successful.

D Performance Profiles for Different β Updates

Figure 8: Performance profile of Algorithm 4 using the second choice of β_i . The same test set is used as in Figure 5.

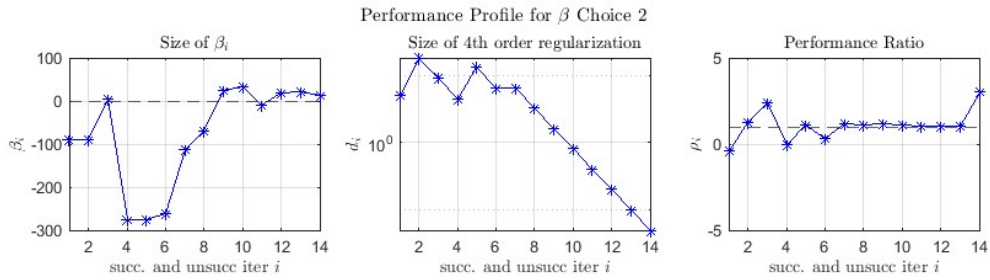
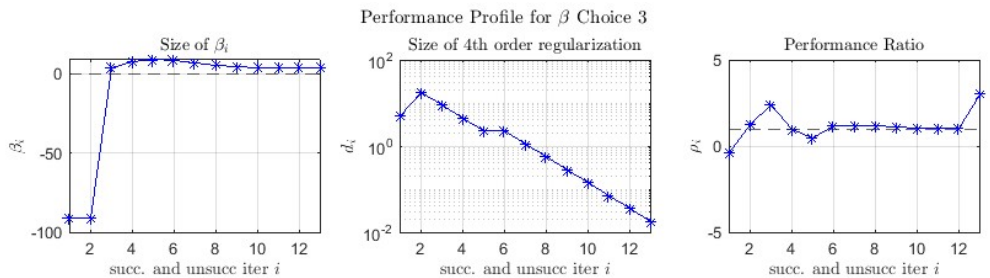


Figure 9: Performance profile of Algorithm 4 using the third choice of β_i . The same test set is used as in Figure 5.



E Numerical Results for Various Test Sets

The results presented in each table are obtained over 10 random problems randomized using MATLAB functions `rand()` or `randn()`. In all of the test cases, all algorithms converge to a point that satisfies $\|g_i\| < \epsilon$ with $\epsilon = 10^{-5}$. The *relative minimum values* of a method are obtained by dividing the minimum value achieved by this algorithm by the minimum of all the minimum values obtained by all algorithms.

Table 2: **Convex m_3 and Convex H** : parameters in (46) are $\mathbf{a} = 80$, and $\sigma = 80$. In the **first part of the table**, m_3 is convex, $H = \text{symm}(30*(\text{randn}(n)+\text{neye}(n)))$ and $\mathbf{c} = 1$; In the **second part of the table**, m_3 is nonconvex but locally convex at $s = \mathbf{0}$, $H = \text{symm}(30*(\text{randn}(n)+\text{neye}(n)))$ and $\mathbf{c} = 80$.

Method	Relative Min.			Iterations.			Evaluations.		
	$n = 5$	50	100	5	50	100	5	50	100
ARC	1	1	1	5.5	3	3	5.5	3	3
Nesterov	1	1	1	12.9	14	15	12.9	14	15
QQR-v1	1	1	1	8.8	9	9	8.8	9	9
QQR-v2	1	1	1	2.9	2	2	2.9	2	2
CQR-choice 2	1	1	1	2.9	2	2	2.9	2	2
CQR-choice 3	1	1	1	2.9	2	2	2.9	2	2
ARC	1	1	1	5.6	4	4	5.6	4	4
QQR-v1	1	1	1	8.8	9	9	8.8	9	9
QQR-v2	1	1	1	4	3	3	4	3	3
CQR-choice 2	1	1	1	4.9	3	3	4.7	3	3
CQR-choice 3	1	1	1	4.7	3	3	4.7	3	3

Table 3: **Ill-Conditioned H , Diagonal H or Singular H** : parameters in (46) are $\mathbf{a} = 80$, $\mathbf{c} = 80$ and $\sigma = 80$. H is a diagonal ill-conditioned matrix with diagonal entries uniformly distributed in $[-10^{-10}, 10^{10}]$.

Method	Relative Min.			Iterations.			Evaluations.		
	$n = 5$	50	100	5	50	100	5	50	100
ARC	1	1	0.99033	9.6	8.6	9.3	6.5	5.7	6
QQR-v1	1	1	0.99033	9	9.7	10.2	8.8	8.6	9.2
QQR-v2	1	1	0.99033	4.1	5	4.7	4.1	4.9	4.5
CQR-choice 2	1	1	1	4.9	7.5	6.5	4.4	5.3	4.7
CQR-choice 3	1	1	0.99033	4.7	5.6	5.7	4.1	4.7	4.5

Table 4: **Changing σ** : From top to bottom, parameters in (46) are $\mathbf{a} = 80$, $\mathbf{b} = 80$, $\mathbf{c} = 80$ and $\sigma = 5, 300$, respectively. The experiments show the algorithm’s ability to handle a range of σ values. Generally, smaller values of σ for $m_3(s)$ require more function/derivative evaluations for convergence across all algorithms.

Method	Relative Min.			Iterations.			Evaluations.		
	$n = 5$	50	100	5	50	100	5	50	100
ARC	1	1	0.98313	11.8	21.7	26.3	8.1	15.1	20.5
QQR-v1	1	0.9958	1	14.5	19.6	22	12.5	17.3	19.5
QQR-v2	1	0.9958	0.97191	8.4	14	16.5	7.6	12.1	14.4
CQR-Choice 2	1	1	0.98498	8.2	15.8	17.5	7	12	15.5
CQR-Choice 3	1	1	0.97191	8.2	13.1	18.8	7.2	11.8	14.8
ARC	1	1	0.99642	12.5	18.4	19.2	6.5	8.5	12.2
QQR-v1	1	1	0.99825	9.9	12.6	16.5	8.5	11.8	15.3
QQR-v2	1	1	1	4.9	7.6	10	4.9	7.4	9.7
CQR-Choice 2	1	1	0.99642	4.9	10.7	11.2	4.9	7.1	9.6
CQR-Choice 3	1	1	0.99642	4.8	7	16	4.8	7	9.8

Table 5: **Large Tensor Term**: parameters in (46) are $\mathbf{a} = 80$, $\mathbf{b} = 80$, $\sigma = 5$, and $\mathbf{c} = 300$ respectively. Minimizing $m_3(s)$ becomes progressively harder with a larger tensor term.

Method	Relative Min.			Iterations.			Evaluations.		
	$n = 5$	50	100	5	50	100	5	50	100
ARC	1	1	0.9845	16.7	24.3	35.1	9.1	15.8	27.1
QQR-v1	0.99204	0.94926	1	18.3	22.1	25.6	15.2	18.6	22.4
QQR-v2	1	1	0.96128	10.6	18.2	22.1	8.4	12.6	18
CQR-Choice 2	1	1	0.98301	10.8	15.4	22	8.3	13.1	19.1
CQR-Choice 3	1	1	0.98301	11.2	20.9	19.6	9	13.2	17.3

Table 6: **Directional and Diagonal Tensors:** In the **first table**, g and T are negative and directional and H is near zero where $g = -80*\text{rand}(n,1)$ and $T = -80*\text{symm}(\text{rand}(n,n,n))$. The parameters in (46) are $b = 0.1$ and $\sigma = 80$. In the **second table**, we consider positive and directional tensors, where parameters in (46) are $a = 80$, $b = 80$, $\sigma = 80$ and T is a diagonal tensor with entries that are uniformly distributed in the range of $[0, 40]$.

Method	Relative Min.			Iterations.			Evaluations.		
	$n = 5$	50	100	5	50	100	5	50	100
ARC	1	1	1	13.2	17.4	15.4	7.1	8.9	7.7
QQR-v1	1	1	1	11.7	19.3	21.1	10.5	15.3	16.6
QQR-v2	1	1	1	6.2	8.7	12.1	6.1	7.3	8.2
CQR-Choice 2	1	1	1	10.4	8.7	8	5.7	7.7	8
CQR-Choice 3	1	1	1	6.7	8.4	11.2	6.1	7.4	8
ARC	1	1	1	11.1	12.5	16.4	6.2	6.5	8
QQR-v1	1	1	1	10.1	10.5	10.4	8.7	8.9	8.4
QQR-v2	1	1	1	4.1	4.4	4.1	4.1	4.4	4.1
CQR-Choice 2	1	1	1	8.3	5.4	5.2	4.9	5.4	5.2
CQR-Choice 3	1	1	1	4.9	5.4	5.2	4.9	5.4	5.2

F More Examples of Badly Scaled Subproblems

Figure 10: **Examples with varying magnitudes of small entries:** In these tests, the setup is the same as in Figure 7 with $n = 99$. The left two plots depict scenarios where the other entries follow a standard normal distribution $\mathcal{N}(0, 1)$. In the right two plots, all other entries, except the first one, are set to zero.

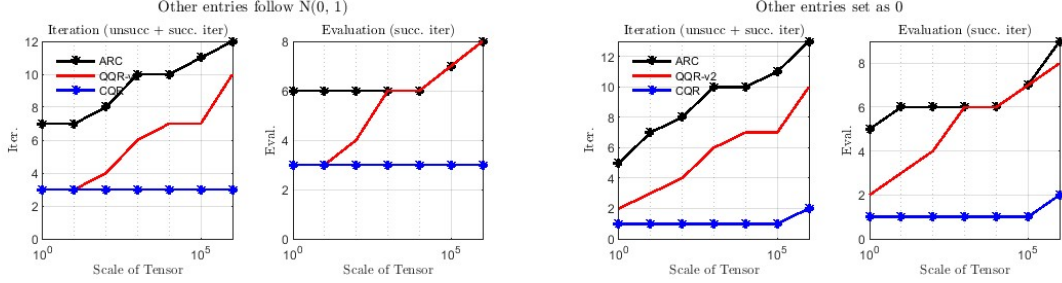


Figure 11: **Examples with different β Choices:** These scenarios use the same setup as in Figure 7, but β_i is chosen according to choice 3. Similar performance advantages are observed.

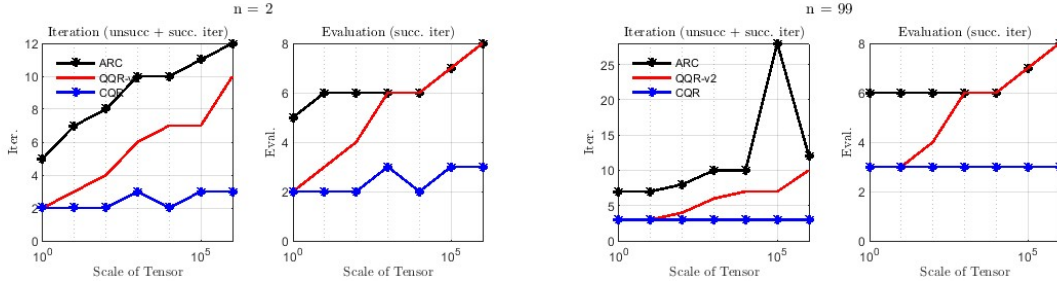
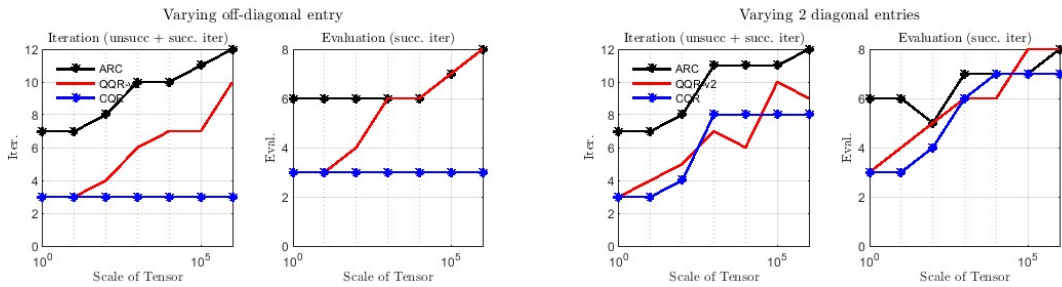


Figure 12: **Examples with multiple large entries:** These tests maintain the same setup as in Figure 7, with $n = 99$. In the left two plots, apart from the first entry diagonal of T , the size of certain off-diagonal entries, such as $T[2, 3, 4]$ and its permutations, also varies from -0.1 to -10^5 . In the right two plots, aside from the first diagonal entry of T , the size of two diagonal entries of T is also varied from -0.1 to -10^5 .



References

- [1] Amir Ali Ahmadi, Abraar Chaudhry, and Jeffrey Zhang. Higher-order newton methods with polynomial work per iteration. *arXiv preprint arXiv:2311.06374*, 2023.
- [2] Orhan Arıkan, Regina S Burachik, and C Yalçın Kaya. Steklov regularization and trajectory methods for univariate global optimization. *Journal of Global Optimization*, 76(1):91–120, 2020.
- [3] Eduardo G Birgin, José M Martínez, and Marcos Raydan. On the use of third-order models with fourth-order regularization for unconstrained optimization. *Computational Optimization and Applications*, 68(3):599–622, 2017.

- [4] Ernesto G Birgin, JL Gardenghi, José Mario Martínez, Sandra Augusta Santos, and Ph L Toint. Worst-case evaluation complexity for unconstrained nonlinear optimization using high-order regularized models. *Mathematical Programming*, 163(1):359–368, 2017.
- [5] Regina S Burachik and C Yalçın Kaya. Steklov convexification and a trajectory method for global optimization of multivariate quartic polynomials. *Mathematical Programming*, 189(1):187–216, 2021.
- [6] Coralia Cartis, Jaroslav M Fowkes, and Nicholas IM Gould. Branching and bounding improvements for global optimization algorithms with lipschitz continuity properties. *Journal of Global Optimization*, 61(3):429–457, 2015.
- [7] Coralia Cartis, Nicholas Ian Mark Gould, and Ph L Toint. Evaluation complexity of algorithms for nonconvex optimization. *MOS-SIAM Series on Optimization.*, 2022.
- [8] Coralia Cartis, Nicholas IM Gould, and Philippe L Toint. Adaptive cubic regularisation methods for unconstrained optimization. part i: motivation, convergence and numerical results. *Mathematical Programming*, 127(2):245–295, 2011.
- [9] Coralia Cartis, Nicholas IM Gould, and Philippe L Toint. Adaptive cubic regularisation methods for unconstrained optimization. part ii: worst-case function-and derivative-evaluation complexity. *Mathematical programming*, 130(2):295–319, 2011.
- [10] Coralia Cartis, Nicholas IM Gould, and Philippe L Toint. Sharp worst-case evaluation complexity bounds for arbitrary-order nonconvex optimization with inexpensive constraints. *SIAM Journal on Optimization*, 30(1):513–541, 2020.
- [11] Coralia Cartis, Nick I Gould, and Philippe L Toint. Universal regularization methods: varying the power, the smoothness and the accuracy. *SIAM Journal on Optimization*, 29(1):595–615, 2019.
- [12] Coralia Cartis, Nick IM Gould, and Ph L Toint. A concise second-order complexity analysis for unconstrained optimization using high-order regularized models. *Optimization Methods and Software*, 35(2):243–256, 2020.
- [13] Coralia Cartis and Lindon Roberts. Scalable subspace methods for derivative-free nonlinear least-squares optimization. *arXiv preprint arXiv:2102.12016*, 2021.
- [14] Coralia Cartis and Wenqi Zhu. Second-order methods for quartically-regularised cubic polynomials, with applications to high-order tensor methods. *arXiv preprint arXiv:2308.15336*, 2023.
- [15] T. Chow. *Derivative and Secant Tensor Methods for Unconstrained Optimization*. PhD thesis, University of California, Berkeley, 1989.
- [16] Andrew R Conn, Nicholas IM Gould, and Philippe L Toint. *Trust region methods*. SIAM, 2000.
- [17] Jean-Pierre Dussault. Arcq: a new adaptive regularization by cubics. *Optimization Methods and Software*, 33(2):322–335, 2018.
- [18] Nicholas IM Gould, Margherita Porcelli, and Philippe L Toint. Updating the regularization parameter in the adaptive cubic regularization algorithm. *Computational optimization and applications*, 53:1–22, 2012.
- [19] Geovani N Grapiglia, Jinyun Yuan, and Ya-xiang Yuan. On the convergence and worst-case complexity of trust-region and regularization methods for unconstrained optimization. *Mathematical Programming*, 152:491–520, 2015.
- [20] Jonas Moritz Kohler and Aurelien Lucchi. Sub-sampled cubic regularization for non-convex optimization. In *International Conference on Machine Learning*, pages 1895–1904. PMLR, 2017.
- [21] Jean B Lasserre. Global optimization with polynomials and the problem of moments. *SIAM Journal on optimization*, 11(3):796–817, 2001.
- [22] Jean Bernard Lasserre. *An introduction to polynomial and semi-algebraic optimization*, volume 52. Cambridge University Press, 2015.
- [23] Monique Laurent. Sums of squares, moment matrices and optimization over polynomials. *Emerging applications of algebraic geometry*, pages 157–270, 2009.
- [24] Zhi-Quan Luo and Shuzhong Zhang. A semidefinite relaxation scheme for multivariate quartic polynomial optimization with quadratic constraints. *SIAM Journal on Optimization*, 20(4):1716–1736, 2010.
- [25] José Mario Martínez and Marcos Raydan. Separable cubic modeling and a trust-region strategy for unconstrained minimization with impact in global optimization. *Journal of Global Optimization*, 63(2):319–342, 2015.

- [26] José Mario Martínez and Marcos Raydan. Cubic-regularization counterpart of a variable-norm trust-region method for unconstrained minimization. *Journal of Global Optimization*, 68:367–385, 2017.
- [27] Jorge J Moré, Burton S Garbow, and Kenneth E Hillstom. Testing unconstrained optimization software. *ACM Transactions on Mathematical Software (TOMS)*, 7(1):17–41, 1981.
- [28] Yurii Nesterov. Implementable tensor methods in unconstrained convex optimization. *Mathematical Programming*, 186(1):157–183, 2021.
- [29] Yurii Nesterov. Inexact accelerated high-order proximal-point methods. *Mathematical Programming*, pages 1–26, 2021.
- [30] Yurii Nesterov. Inexact high-order proximal-point methods with auxiliary search procedure. *SIAM Journal on Optimization*, 31(4):2807–2828, 2021.
- [31] Yurii Nesterov. Superfast second-order methods for unconstrained convex optimization. *Journal of Optimization Theory and Applications*, 191(1):1–30, 2021.
- [32] Yurii Nesterov. Quartic regularity. *arXiv preprint arXiv:2201.04852*, 2022.
- [33] Yurii Nesterov and Boris T Polyak. Cubic regularization of newton method and its global performance. *Mathematical Programming*, 108(1):177–205, 2006.
- [34] Jorge Nocedal and Stephen J Wright. *Numerical optimization*. Springer, 1999.
- [35] Liqun Qi, Zhong Wan, and Yu-Fei Yang. Global minimization of normal quartic polynomials based on global descent directions. *SIAM Journal on Optimization*, 15(1):275–302, 2004.
- [36] Robert B Schnabel. Tensor methods for unconstrained optimization using second derivatives. *Mathematics of Computation*, 25(114):295–315, 1971.
- [37] Robert B Schnabel and Ta-Tung Chow. Tensor methods for unconstrained optimization using second derivatives. *SIAM Journal on Optimization*, 1(3):293–315, 1991.
- [38] Wenqi Zhu and Coralia Cartis. Quartic polynomial sub-problem solutions in tensor methods for nonconvex optimization. In *NeurIPS 2022 Workshop*, 2022.